Magneto-Optical Trapping of Lithium

Erik Anciaux

June 6, 2013

A thesis submitted in partial satisfaction of the requirements for the degree of Bachelor of Science in Physics in the College of Creative Studies of the University of California Santa Barbara

Thesis Advisor: David Weld

This thesis of Erik Anciaux is approved

_____ _____

David Weld, Advisor Date

Abstract

Magneto-optical trapping is a method of trapping and cooling atoms consisting of three pairs of counter propagating laser beams aimed at a sample of gaseous atoms. Using further techniques including Sisyphus cooling and evaporative cooling, the atoms will enter a state of quantum degeneracy. Our setup consists of an atomic lithium beam fired from an oven, slowed by a Zeeman slower and collimated using transverse laser cooling such that the atomic beam is sufficiently narrow and slow to be trapped by the magneto-optical trap. This thesis will focus on the transverse cooling apparatus as well as the modular optics of the magneto-optical trap.

Acknowledgments

First and foremost I would like to thank my research advisor, Dr. David Weld, for hiring me on as an undergraduate researcher and for providing constant mentorship for the past year. David introduced me to atomic physics and helped me learn about the field and about scientific research in general. He was an outstanding mentor and advisor and has shown great care for the development of all of his students, both as scientists and as people.

I would also like to thank the members of the Weld Lab with whom I have worked with over the past year for their advice, collaboration and friendship including Shankari Rajagopal, Zach Geiger, Ruwan Senaratne, Slava Lebedev, Kurt Fujiwara, Max Garber, Erica Mason, Anne Hebert, Shura Kotlerman, Robert Salazar, Alan Long, Eric Corsini and Dylan Kennedy. The Weld Lab has been an incredible place to learn physics because of the brilliant scientists always willing to help each other and for the friendly and encouraging environment that they have created.

Thank you to all of the UCSB Physics faculty who have taught me over the past four years, especially the CCS Physics faculty who have taught me, mentored me, advised me and even recruited me to UCSB including Ilan Ben-Yaacov, Sathya Guruswamy, Doug Folsom, Francesc Roig and Tengiz Bibliashivli. Also, thanks to Carl Gwinn and Michael Johnson for advising me before I joined the Weld Lab. The College of Creative Studies has been a special place to learn physics and has provided me with a great undergraduate physics education.

Lastly, I would like to thank my parents for supporting my educational endeavors, inspiring me to pursue a career in science and for all of the love and support they have given me over the past 21 years. And for paying for my education.

Contents

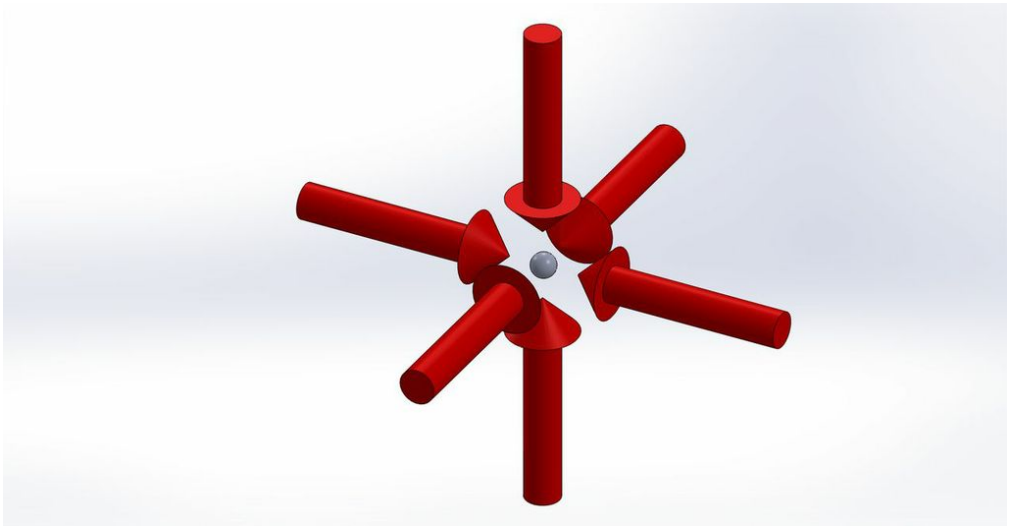

Figure 1: Three sets of counter-propagating beams aimed at a cloud of lithium atoms.

1 Introduction

One of the most fundamental developments in physics over the past century was the development of quantum mechanical theories describing the atomic absorption and emission of light. The emission and absorption depend greatly on the properties of the atoms absorbing the light, the incoming light and the external fields. Our experiment takes advantage of these properties to trap and cool lithium atoms in a magneto-optical trap.

Our experiment uses an oven to gasify solid lithium and a nozzle to collimate the atoms into an atomic beam. The atomic beam is then further collimated using counter propagating lasers, or transverse cooling, to decrease the transverse velocities of the atomic beam. The beam then travels through a Zeeman slower to decrease the longitudinal velocity of the atoms, therefore increasing their divergence before being recollimated by a second round of transverse cooling. The atoms are then collimated and slow and can be trapped using a magneto-optical trap. The trapped atoms can be cooled using further cooling techniques until most atoms are in the ground state, forming a degenerate state of matter.

As the temperature lowers to near absolute zero, the phase space density increases. $\rho = n * \Lambda^3$ where n is density of atoms and the DeBroglie wavelength Γ is defined by

$$\Lambda = \frac{\hbar\sqrt{2\pi}}{\sqrt{mk_bT}}$$

where m is the mass of the atom and T is the temperature. In terms of temperature, this gives

$$\rho = n * \hbar^3 (\frac{2\pi}{mk_bT})^{\frac{3}{2}}$$

If the atoms are bosons, as T decreases to a critical temperature T_c, the phase space density will increase to a critical density $\rho \approx 2.612$, at which point the atoms will enter a phase of matter called a Bose-Einstein condensate. The critical density is equal to the Riemann Zeta function with argument $\frac{3}{2}$.

$$\zeta(\frac{3}{2}) \approx 2.612$$

When $T < T_c$, the wavefunctions of individual atoms will overlap. Because the particles are bosons, multiple may exist in the same state, in this case the ground state. [1]

If the atoms are fermions, the atoms will form a degenerate Fermi gas in which the atoms will fill up all of the ground states below a certain energy,

$$E_{Fermi} = \frac{\hbar^2}{2m}(3\pi^2 n)^{\frac{2}{3}}$$

Our lab hopes to use large samples of lithium atoms in the ground state to conduct experiments in quantum simulations, non-equilibrium dynamics, topological phases and force sensing that could provide insight into problems in solid state physics and quantum computing.

1.1 Stimulated absorption

For a two level atom, the atom can be excited from the ground state to the excited state by absorbing a photon with energy equal to the difference between the ground state energy and the excited state energy. The probability of absorption will be greatest if the energy of the photon $\hbar\omega$ is exactly equal to the difference between the energy of the excited state E_2 and the ground state E_1 and decreases as the difference between the photon energy and the transition energy increases. For notational convenience, we define

$$\omega_0 \equiv \frac{E_2 - E_1}{\hbar}.$$

When an atom in its ground state absorbs a photon, the atom will gain the energy of the photon and become excited. A time later, the atom will emit a photon of the same frequency as the original photon in a random direction and return to its ground state via spontaneous emission. The probability of the atom remaining in the excited state after a time t is given by

$$P_e = e^{-\frac{t}{\tau}}$$

where $\tau = \frac{1}{\Gamma}$ is the lifetime of the excited state. The number of photons absorbed per unit time will be given by a Lorentzian Distribution centered about ω_0 with a full width at half maximum Γ.

$$P = \frac{s_0(\frac{\Gamma}{2})^3}{(\omega - \omega_0)^2 + (s_0 + 1)(\frac{\Gamma}{2})^2}$$

where

$$s_0 = \frac{I}{I_{saturation}}$$

where I is the intensity of the incoming beam and $I_{saturation}$ is the saturation intensity of the atomic transition.[2]

When an atom in its ground state absorbs a photon, the atom will gain the energy of the photon and become excited. A time later, the atom will emit a photon of the same frequency as the original photon in a random direction and return to its ground state via spontaneous emission. The probability of the atom remaining in the excited state after a time t is given by

$$P_e = e^{-\frac{t}{\tau}}$$

where $\tau = \frac{1}{\Gamma}$ is the lifetime of the excited state.

In addition to energy, photons also carry momentum, $\hbar\vec{k}$. The wavevector $\vec{k}$ points in the direction of propagation of the light and has magnitude $\frac{2\pi}{\lambda}$. When the atom absorbs the photon, it receives a momentum kick $\hbar\vec{k}$ from the photon. When the atom emits a photon, it will receive a momentum kick in the opposite direction of the emitted photon equal and opposite to the photon momentum due to Newton's third law.

The net change in momentum of the atom after absorbing and emitting one photon will be

$$\Delta\vec{p} = \hbar(\vec{k} - \vec{k'})$$

where $\vec{k}$ is the wavevector of the incoming photon and $\vec{k'}$ is the wavevector of the outgoing photon. Because the direction of the emitted photon is random, the expectation value of the change in momentum will be

$$< \Delta\vec{p} >= \hbar\vec{k}$$

[3]

1.2 Doppler Shift

If an atom is moving with respect to the source of an incoming beam, the frequency of the incoming beam in the atom's frame will be shifted by

$$\Delta\omega = \frac{-\omega_i \vec{v} \cdot \hat{n}}{c}$$

where ω_i is the frequency of the incoming light in the lab frame and $\Delta\omega$ is the shift in frequency. Replacing $\frac{\omega_i}{c}\hat{n}$ with $\vec{k}$ gives

$$\Delta\omega = -\vec{v} \cdot \vec{k}$$

This means that a moving atom will only absorb photons with frequency near $\omega = \omega_0 + \vec{v} \cdot \vec{k}$. For notational convenience, we donate $\omega - \omega_0$ by δ. The scattering rate of the atom absorbing a photon will be

$$P = \frac{s_0(\frac{\Gamma}{2})^3}{(\delta - \vec{v} \cdot \vec{k})^2 + (s_0 + 1)(\frac{\Gamma}{2})^2}$$

The scattering rate will be maximized when

$$(\delta - \vec{v} \cdot \vec{k})^2 \approx 0$$

and will be negligible if

$$(\delta - \vec{v} \cdot \vec{k})^2 \gg (\frac{\Gamma}{2})^2$$

P is defined in units of cycles per second.

The beam will be most likely to interact with the atom if the light is detuned from the resonant frequency of the transition by a frequency $\vec{v} \cdot \vec{k}$. Red detuned light will be more likely to be absorbed by atoms moving opposite to the direction of the beam and blue detuned light will be more likely to interact with atoms moving in the same direction as the beam. The atom will be most likely to absorb the photon if the difference between the frequency of the laser light is within the range

$$\frac{\omega_0 \vec{v} \cdot \hat{n}}{c} - \frac{\Gamma}{2} < \delta < \frac{\omega_0 \vec{v} \cdot \hat{n}}{c} + \frac{\Gamma}{2}$$

1.3 Optical Forces

When the incoming photon excites an atom, it provides a momentum kick in the direction of the beam given by

$$\Delta\vec{p} = \hbar\vec{k}$$

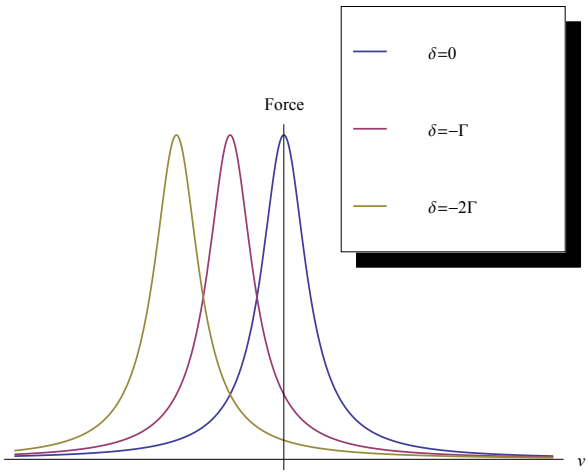

Figure 2: This graph shows the expectation value of the Doppler force versus atomic velocity of one beam on an atom for various values of the detuning δ. If the incoming beam is not detuned, the net force will be the same for atoms moving towards the beam as atoms moving away from the beam. If the red detuning is equal to the linewidth, $\delta = -\Gamma$, the net force will be greatest for atoms moving towards the laser with $\vec{v} \cdot \vec{k} = -\Gamma$ and will have a full width at half maximum Γ. For a red detuning, $\delta = -2\Gamma$, the net force on atoms will be greatest for atoms moving towards the laser with $\vec{v} \cdot \vec{k} = -2\Gamma$ and will also have a full width at half maximum Γ.

After N excitation and relaxation cycles,

$$\Delta\vec{p} = N\hbar\vec{k}$$

where N is the total number of momentum kicks. The average force exerted by an incoming laser beam on an atom is equal to the total momentum change per unit time.

$$\vec{F} = \frac{\Delta\vec{p}}{\Delta t} = \frac{N}{\Delta t}\hbar\vec{k}$$

Replacing $\frac{N}{\Delta t}$ with P from Section 1.2 gives

$$\vec{F} = P\hbar\vec{k} = \frac{s_0(\frac{\Gamma}{2})^3\hbar\vec{k}}{(\delta - \vec{v} \cdot \vec{k})^2 + (s_0 + 1)(\frac{\Gamma}{2})^2}$$

This gives the optical force on an atom as a function of its velocity. Both Γ and δ are constants determined by the properties of atom and the laser. The force will be greatest within the range

$$\delta - \frac{\Gamma}{2} < \vec{v} \cdot \vec{k} < \delta + \frac{\Gamma}{2}$$

and decrease to zero as $\vec{v} \cdot \vec{k}$ goes beyond this range.

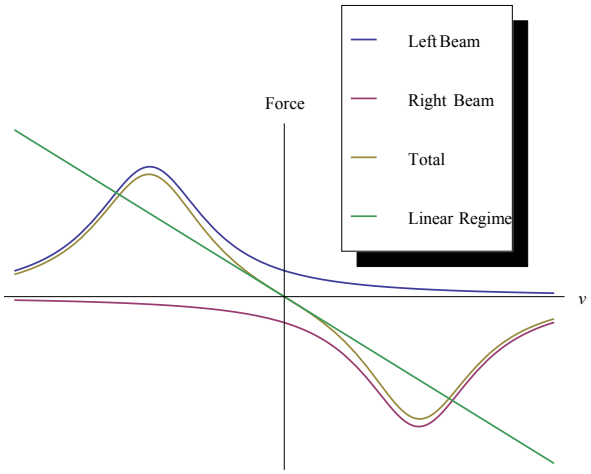

Figure 3: This graph shows the expectation value of the force on an atom with speed v due to beams detuned by $\delta = -\Gamma$ incoming from the left and right as well as the sum of the forces. The net force is linear for small v.

1.4 Counter-propagating beams

If two beams of identical intensity and frequency are counter-propagating, they will each apply a velocity dependent Doppler force to atoms

$$\vec{F} = \frac{s_0(\frac{\Gamma}{2})^3\hbar\vec{k}}{(\delta - \vec{v}\cdot\vec{k})^2 + (s_0+1)(\frac{\Gamma}{2})^2} + \frac{-s_0(\frac{\Gamma}{2})^3 C\hbar\vec{k}}{(\delta + \vec{v}\cdot\vec{k})^2 + (s_0+1)(\frac{\Gamma}{2})^2}$$

$$\vec{F} = s_0(\frac{\Gamma}{2})^3\hbar\vec{k}\frac{((\delta + \vec{v}\cdot\vec{k})^2 + (\frac{\Gamma}{2})^2) - ((\delta - \vec{v}\cdot\vec{k})^2 + (\frac{\Gamma}{2})^2)}{((\delta - \vec{v}\cdot\vec{k})^2 + (s_0+1)(\frac{\Gamma}{2})^2)((\delta + \vec{v}\cdot\vec{k})^2 + (s_0+1)(\frac{\Gamma}{2})^2)}$$

$$\vec{F} = s_0(\frac{\Gamma}{2})^3\hbar\vec{k}\frac{(\delta + \vec{v}\cdot\vec{k})^2 - (\delta - \vec{v}\cdot\vec{k})^2}{((\delta - \vec{v}\cdot\vec{k})^2 + (s_0+1)(\frac{\Gamma}{2})^2)((\delta + \vec{v}\cdot\vec{k})^2 + (s_0+1)(\frac{\Gamma}{2})^2)}$$

Taylor Expanding around $\vec{v}\cdot\vec{k} = 0$ gives

$$\vec{F} = s_0(\frac{\Gamma}{2})^3\hbar\vec{k}\frac{4\vec{v}\cdot\vec{k}\delta}{(\delta^2 + (s_0+1)(\frac{\Gamma}{2})^2)^2}$$

$$\vec{F} = s_0\Gamma^3\hbar\vec{k}\frac{\vec{v}\cdot\vec{k}\delta}{2(\delta^2 + (s_0+1)(\frac{\Gamma}{2})^2)^2}$$

If the beam is red detuned, $\delta < 0$ and the force will be damping. The detuning δ shall be set

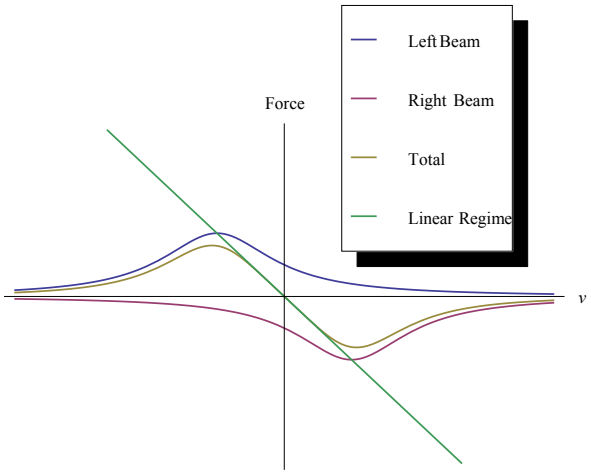

Figure 4: This graph shows the expectation value of the force on an atom with speed v due to beams detuned by $\delta = -\frac{\Gamma}{2}$ incoming from the left and right as well as the sum of the forces. The net force is linear for a larger range of values of v. The optimum detuning will be $\delta = -\frac{\Gamma}{2}$.

equal to $\frac{\Gamma}{2}$ to maximize the range of the linear regime.

The net result of Doppler cooling will be the reduction of kinetic energy and temperature to the Doppler limit, which corresponds to the energy range of photons within the linewidth.

$$E = \hbar\frac{\Gamma}{2} = k_b T_{Doppler}$$

or

$$T_{Doppler} = \frac{\hbar\Gamma}{2k_b}$$

[4]

Optical molasses contains the three dimensional analog of this setup, with pairs of counter propagating beams aligned at right angles to each other. Each pair of beams will control the velocity in the axial direction of the beams and reduce the velocity in that direction to the Doppler limit. The result will be a cloud of slow, cold atoms centered around the intersection of the three pairs of beams.[5]

2 Transverse Cooling

In order to prepare a trappable dilute gas of lithium atoms, the atoms must be evaporated from their natural solid state and transported into a vacuum chamber. The first step in this process is heating the lithium using an oven. The oven will gasify the atoms which will then have a large mean velocity and escape through a nozzle toward the vacuum chamber. After

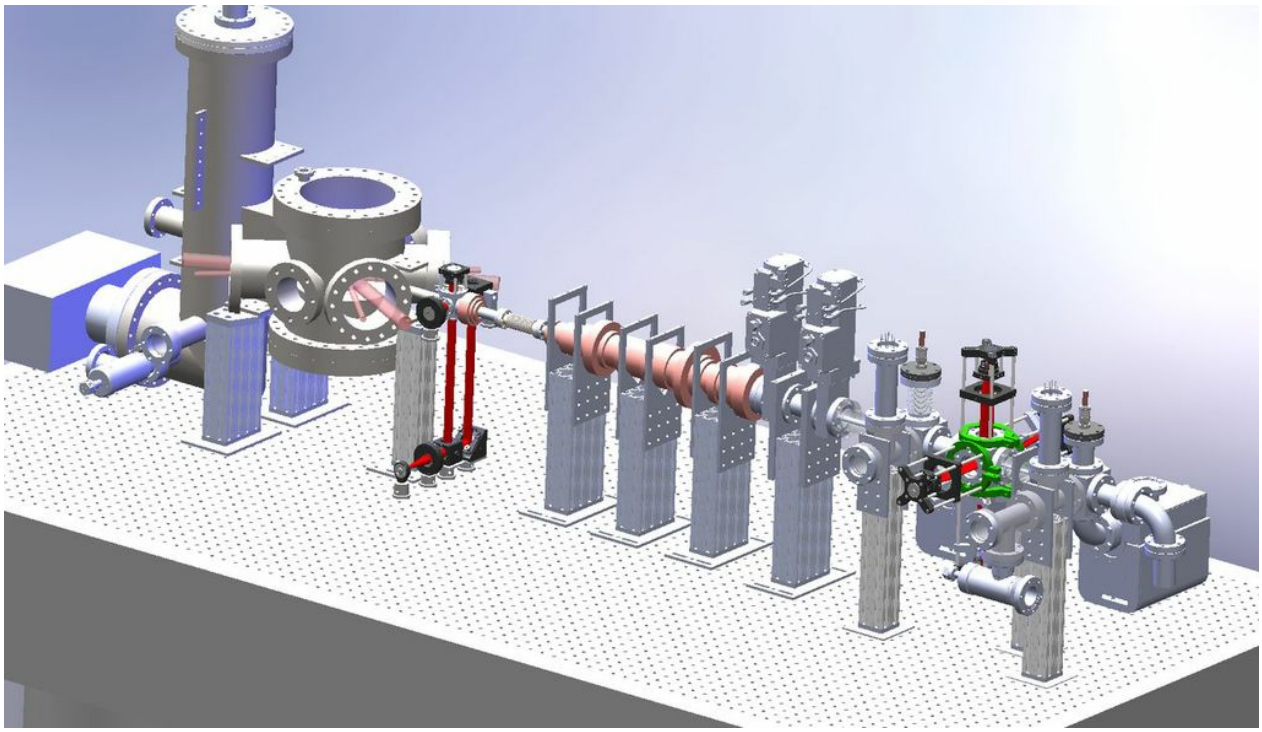

Figure 5: This is the optical table featuring the path of the atom from right to left from the oven through the fast beam transverse cooling apparatus, through the Zeeman slower, slow beam transverse cooling apparatus into the vacuum chamber. Design Credit: Zach Geiger, Shankari Rajagopal, Ruwan Senaratne, Erik Anciaux

escaping, the atomic beam will have a finite divergence. The beam can be further collimated by using transverse cooling, which is a two dimensional analog of optical molasses. The transverse cooling decreases the transverse velocity of the atomic beam, minimizing beam expansion. Next the atomic beams enters a Zeeman slower which uses a spatially varying magnetic field and a counter-propagating laser to slow the longitudinal atomic beam speed. As the atoms are slowed, the angle of divergence increases because the longitudinal velocity decreases, but the transverse velocity does not. This requires another transverse cooling process to collimate the atomic beam such that atoms are sufficiently slow and sufficiently near the trap to be trapped by the magneto-optical trap.

This section will focus on the mechanics of the transverse cooling apparatuses, designed by Erik Anciaux. The oven and Zeeman slower were designed and made by Ruwan Senaratne, Zach Geiger, and David Weld.

2.1 Theory

Transverse cooling utilizes the same physics as Doppler cooling in two dimensions. The apparatus is set up with two sets of counter-propagating laser beams orthogonal to each other and orthogonal to the atomic beam. The atomic beam and the centers of the two sets

of counter-propagating beams intersect at one point. The width of the laser beams must be at least as wide as the atomic beam in the direction normal to the beam, but any power delivered outside the width of the atomic beam will be wasted. The width of the beams in the direction of the atomic beam propagation must be sufficiently wide to provide enough time for the beams to cool the transverse velocity of the atomic beam to the Doppler Limit. The beams should be detuned from resonance by $\frac{\Gamma}{2}$ in order to apply a Doppler force to atoms moving with near zero velocity against the direction of the laser beam, but not apply any force to atoms with transverse velocities in the same direction as the laser beam.

2.1.1 Lin $\perp$ Lin

For each set of counter-propagating beams, the polarization must be configured such that each beam has orthogonal linear polarization. This causes a spatially varying electric field along the axis of the laser beam allowing the transverse velocities of the atomic beam to cool below the Doppler limit. The electric fields of the two counter-propagating beams add. Because the beams are traveling in opposite directions, even though each individual polarization direction is constant, the direction and magnitude of the total electric field shifts. Throughout the course of one half wavelength in space, the phase of the standing wave changes from linear in one direction to circularly polarized, to linear in the opposite direction to circularly polarized in the opposite direction, back to linear in the initial direction. Between the extreme case scenarios of perfectly linear or circularly polarization, the net polarization of the standing wave will shift through elliptical polarizations. [6]

This can be derived by treating the electric fields of the two counter-propagating electric fields. Let the incoming beam be represented by

$$E_1 = E_0 e^{i(\omega t - kz)} \hat{x}$$

and the counter-propagating beam be represented by

$$E_2 = E_0 e^{i(\omega t + kz)} \hat{y}$$

Summing the two electric fields gives

$$E_{total} = E_1 + E_2 = E_0 e^{i(\omega t - kz)} \hat{x} + E_0 e^{i(\omega t + kz)} \hat{y}$$

$$E_{total} = E_0 e^{i\omega t} (e^{-ikz} \hat{x} + e^{ikz} \hat{y})$$

If $z = n\lambda$,

$$E_{total} = E_0 e^{i\omega t}(e^{-i2n\pi}\hat{x} + e^{i2n\pi}\hat{y}) = E_0 e^{i\omega t}(\hat{x} + \hat{y})$$

which is the equation for the Electric field of light polarized in the $\hat{i} + \hat{j}$ direction.
If $z = n\lambda + \frac{\lambda}{8}$,

$$E_{total} = E_0 e^{i\omega t}(e^{-i(2n\pi + \frac{\pi}{4})}\hat{x} + e^{i(2n\pi + \frac{\pi}{4})}\hat{y}) = E_0 e^{i\omega t}(e^{-i\frac{\pi}{4}}\hat{x} + e^{i\frac{\pi}{4}}\hat{y})$$

$$= E_0 e^{i\omega t} e^{-i\frac{\pi}{4}}(\hat{x} + e^{i\frac{\pi}{2}}\hat{y}) = E_0 e^{i\omega t} e^{-i\frac{\pi}{4}}(\hat{x} + i\hat{y})$$

which is the equation for the Electric field of counterclockwise circularly polarized light.
If $z = n\lambda + \frac{\lambda}{4}$,

$$E_{total} = E_0 e^{i\omega t}(e^{-i(2n\pi + \frac{\pi}{2})}\hat{x} + e^{i(2n\pi + \frac{\pi}{2})}\hat{y}) = E_0 e^{i\omega t}(e^{-i\frac{\pi}{2}}\hat{x} + e^{i\frac{\pi}{2}}\hat{y})$$

$$= E_0 e^{i\omega t} e^{-i\frac{\pi}{2}}(\hat{x} + e^{i\pi}\hat{y}) = -E_0 e^{i\omega t}(\hat{x} - \hat{y})$$

which is the equation for the Electric field of light polarized in the $(\hat{x} - \hat{y})$ direction.
If $z = n\lambda + \frac{3\lambda}{8}$,

$$E_{total} = E_0 e^{i\omega t}(e^{-i(2n\pi + \frac{3\pi}{4})}\hat{x} + e^{i(2n\pi + \frac{3\pi}{4})}\hat{y}) = E_0 e^{i\omega t}(e^{-i\frac{3\pi}{4}}\hat{x} + e^{i\frac{3\pi}{4}}\hat{y})$$

$$= E_0 e^{i\omega t} e^{-i\frac{3\pi}{4}}(\hat{x} + e^{i\frac{3\pi}{2}}\hat{y}) = E_0 e^{i\omega t} e^{-i\frac{3\pi}{4}}(\hat{x} - i\hat{y})$$

which is the equation for the Electric field of clockwise circularly polarized light.
If $z = n\lambda + \frac{\lambda}{2}$,

$$E_{total} = E_0 e^{i\omega t}(e^{-i(2n\pi + \pi)}\hat{x} + e^{i(2n\pi + \pi)}\hat{y}) = E_0 e^{i\omega t}(e^{-i\pi}\hat{x} + e^{i\pi}\hat{y})$$

$$= E_0 e^{i\omega t} e^{-i\pi}(\hat{x} + e^{2i\pi}\hat{y}) = -E_0 e^{i\omega t}(\hat{x} + \hat{y})$$

which is the equation for the Electric field of light polarized in the $\hat{x} + \hat{y}$ direction, similar to the light at $z = n\lambda$. The cycle will repeat again as z increases.

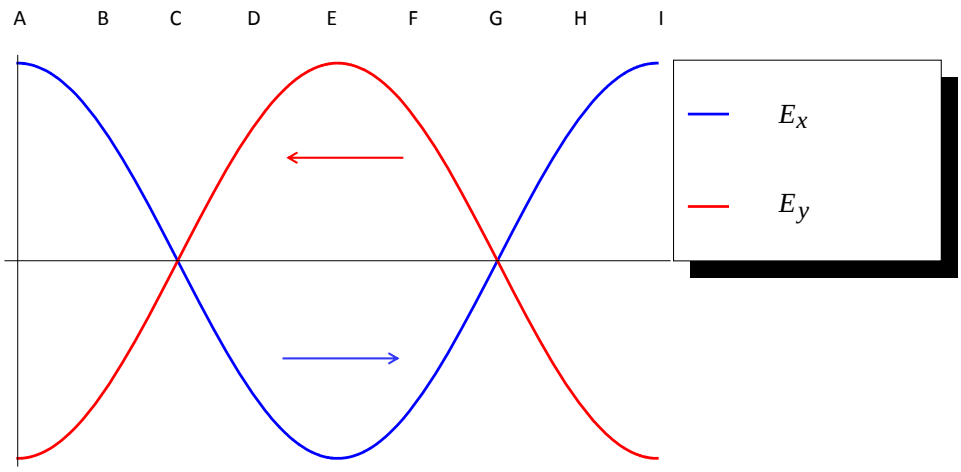

Figure 6: This graph shows the spatially varying polarization of two counter-propagating waves polarized in the $\hat{x}$ and $\hat{y}$ directions over the course of one wavelength. In figure 6, at point A, the light will be linearly polarized in the $\hat{x} - \hat{y}$ direction. At point B, the light will be right handed circularly polarized. At point C, the light will be linearly polarized in the $\hat{x} + \hat{y}$ direction. At point D, light will be left handed circularly polarized. A point E, the light will be linearly polarized in the $\hat{x} - \hat{y}$ direction. At point F, the light will be right handed circularly polarized. At point G, the light will be linearly polarized in the $\hat{x} + \hat{y}$ direction. At point H, light will be left handed circularly polarized and at point I, the light will be linearly polarized in the $\hat{x} - \hat{y}$ direction. The polarization can be determined by considering the progression of the electric field vector as a function of time at a given location.

The spatial polarizarion gradient causes a change in the energy of the ground state of the atom based on the position of the atom. The degeneracy of the ground state will also be lifted such that a specific position can correspond to two or more different ground state energies. When the ground state energy is greater than the zero electric field energy, the transition energy between the ground state and excited state will be less than the zero electric field transition energy, therefore a beam red detuned from resonance will be more likely to excite an atom from the ground state with greater energy. After absorbing the photon, the atom will emit a photon and return to the same ground state, or to the lower energy ground state. If it returns to the original ground state, there will be no energy loss, but if it returns to the lower energy ground state, the atom will lose energy equivalent to the difference in energy between the original ground state energy and the final ground state energy. The atom will then move through the field until it is again at a point of maximum ground state energy, where the cycle will repeat. After a sufficient number of cycles, the atom will not have the kinetic energy necessary to travel to a point with maximum ground state energy and will not be able to be excited by the incoming photon. This process is a form of polarization gradient cooling. See Section 3.1.2 for further description of polarization gradient cooling.

2.1.2 Fast Beam Cooling

After the atoms leave the oven and before they reach the Zeeman slower, they are moving with speeds of several hundred meters per second through the transverse cooling apparatus, meaning that the atoms will enter and exit the laser beam intersection very rapidly. In order for the cooling procedure to be optimized, the number of photon absorption emission cycles must be sufficient to cool the atoms to the Doppler limit. In order to optimize the number of cycles, the time that the atoms spend in the laser beam intersection must be optimized, which means the distance the atoms travel through the beams must also be optimized.

The laser beam must be wide enough along the direction of the atomic beam to optimize the transverse cooling, however the vertical width of the laser beam does not need to be any wider than the atomic beam. The most power efficient way to satisfy both criteria is to create elliptical beams with a major axis along the direction of the atomic beam and the minor axis orthogonal to the direction of both the atomic beam and the incoming laser beam.

2.2 Fast Beam Cooling Design

The pre Zeeman slower transverse cooling apparatus acts on the atomic beam as it passes through a cube with six CF275 flanges attached one per side. The optics of the laser beams are attached to the CF flanges using C clamps with cage holes drilled to fit the end of a 60mm Thorlabs cage system for 2" optics. The clamps are circular with inner diameter 2.73"

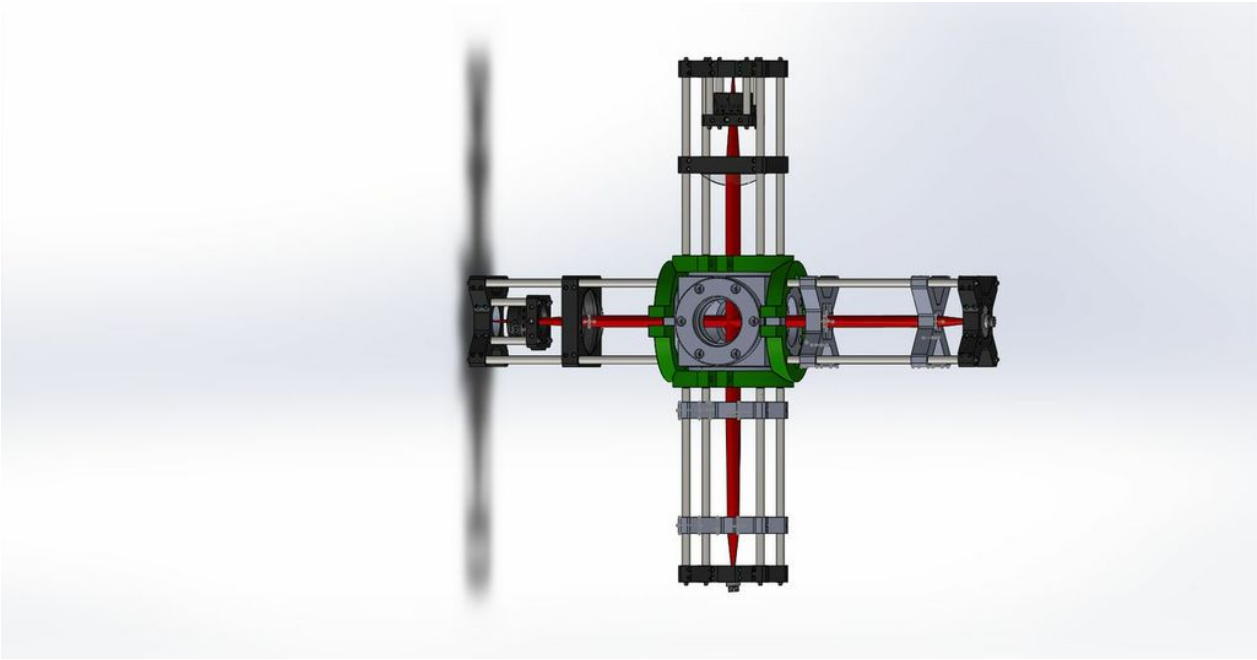

Figure 7: This figure shows the three dimensional representation of the design of the fast beam cooling. Two light sources enter the system through FC/APC patch cables and are elliptically collimated by two sets of cylindrical lenses. The beams travel through the atomic beam before being focused by a 75mm lens to a point on a mirror. Between the lens and mirror lies a quarter wave plate to tilt the direction of the polarization of the beam upon retroreflection. The retroreflected beam then passes back through the atomic beam, creating a lin perp lin polarization.

to fit outside the of the CF flange. The circle is broken at one end to allow the clamp to flex to tighten to the flange. The clamp is tightened to the flange by using a screw to tighten or loosen two flanges jutting from the break in the circle. The clamp has an upper lip .1" thick and .1" deep covering the CF flange to ensure the clamp does not shift in position from the flange. Six holes are drilled into the inside of the clamp to allow space for bolts to be attached to the CF flange.

Four clamps must be attached to CF flanges for each side with an incoming laser beam. The edge of each cube is 2.75" long compared to 2.72" for the diameter of the CF Flange. The thickness and depth of each clamp is .5". Without modifications, clamps on neighboring sides of the cube would overlap. This requires each clamp to be cut at a 45 degree angle on one edge such that the neighboring clamps to do not overlap. The clamping mechanism jutting out from the clamp must point along the atomic beam for each clamp. Because the holes on the CF flanges are rotated on neighboring sides, clamps on neighboring sides must have the bolt holes rotated by 90°. Attached to the clamp via the holes on the front face are Thorlabs cage optics. The cage optics hold the mirrors, waveplates and lenses necessary to shape and direct the beam. Laser light is transported to the cage using optical fiber with FC/APC ends mounted into an FC/APC connector on the cage.

2.2.1 Elliptical Beam Collimation

As the laser beam exits the fiber, it is diverging with a numerical aperture of .11. The width of the atomic beam is 8.8 mm and must travel through the laser beam intersection for 28mm in order to reach the Doppler Limit. This means that a beam profile with height 8.8mm and width 28mm in the direction of atomic beam propagation will collimate the atomic beam with minimal power wasted. The beam can be collimated by placing two cylindrical lenses, one mounted horizontally and one mounted vertically, each separated from the output of the fiber by its focal length to create an elliptical beam. First will be a horizontally mounted 40mm lens, followed by a vertically mounted 130mm lens. The 40mm lens will collimate the vertical axis of the beam while the horizontal axis of the beam will continue to expand before being collimated by the 130mm lens.

The height of the beam exiting the lenses will be twice the numerical aperture multiplied by the first focal length, $2NA * f = 8.8mm$. The width of the beam will be twice the numerical aperture multiplied by the second focal length $2NA * f = 28.6mm$. The beam profile after both lenses will be elliptical with major axis 28.6mm in the direction of propagation of the atomic beam and minor axis 8.8mm along the vertical direction. The major and minor axis dimensions correspond to the $1/e^2$ dropoff from the central maximum of the Gaussian beam.

The cylindrical lenses are mounted to the cage using cylindrical cage mounts. These mounts are similar to Thorlabs 60mm cage plates, but instead of having housing for a circular optic,

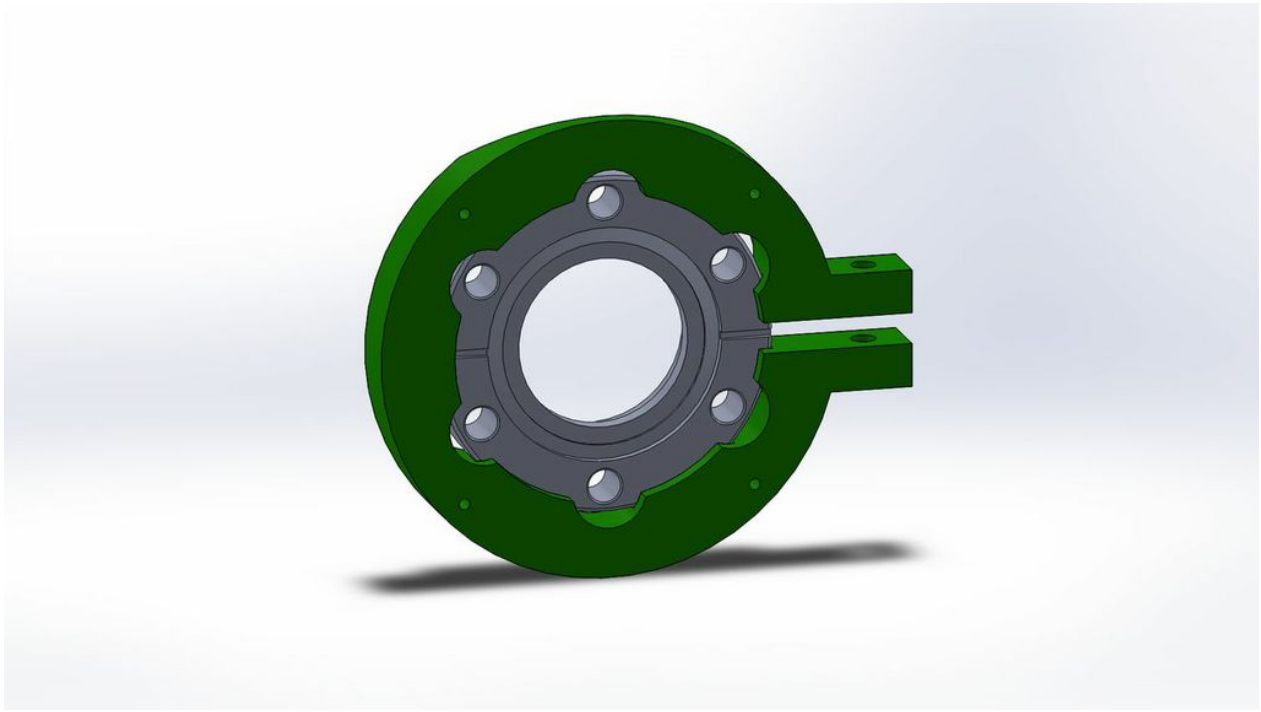

Figure 8: This is a three dimensional representation of the clamp designed to link the cage mounted optics to the CF 275 flange attached to the cube. The clamp rests on the front face of the CF 275 flange with six holes cut from the face of the clamp to allow room for bolts to attach the flange to the cube. The clamp can be tightened or loosened by applying pressure to the two tabs on the right. In order to aviod collisions with clamps on the neighboring faces of the cube, the backside of the clamp is cut at 45° angles at the top and bottom. Four 4-40 holes are drilled into the front face of the clamp in order to attach a 60mm Thorlabs cage system.

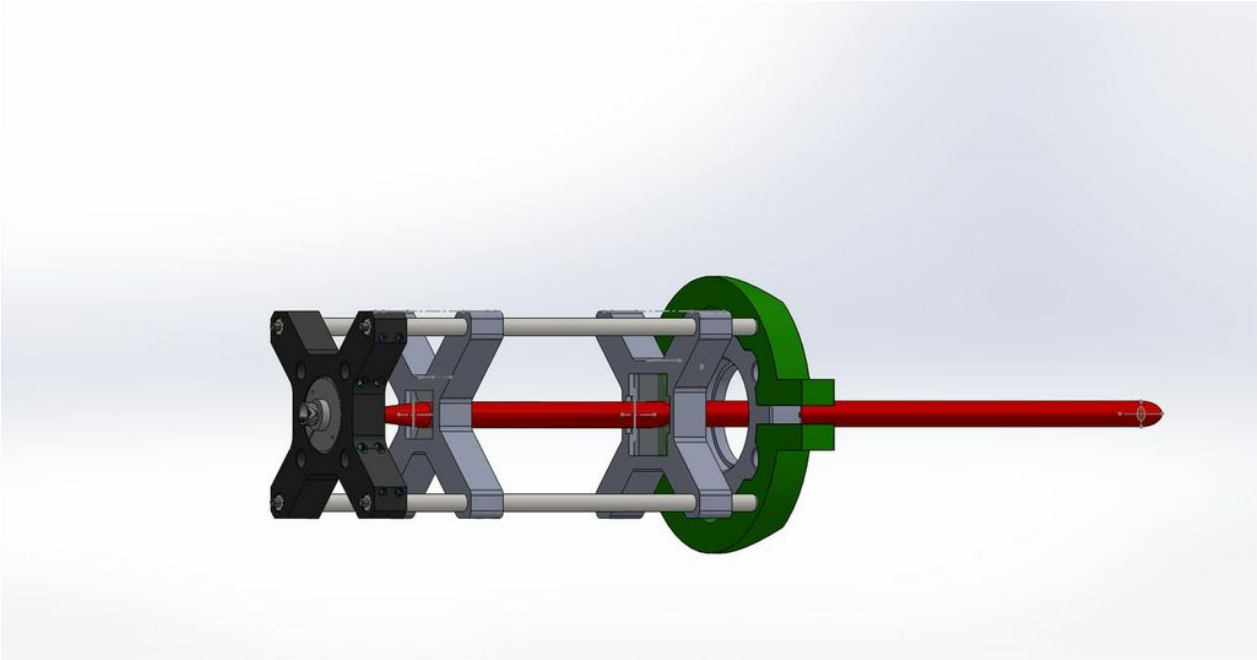

Figure 9: The optics are mounted to the transverse cooling apparatus by using a Thorlabs 60mm cage system. The rods making up the boundary of the cage are attached to a clamp(shown in green) around the CF flange mounted to the transverse cooling cube. The light enters the transverse cooling apparatus through an FC/APC adapter inside a Thorlabs LCP02 cage plate. The light then expands to a 40mm focal length cyndrical lens mounted horizontally inside a custom designed x shaped cage mount, designed to hold cylindrical optics inside a 60mm cage system. The light then expands in the horizontal direction until it passes through a second cylindrical lens of focal length 130mm, this time oriented vertically. The second lens is in a larger x shaped cage mount to account for the larger beam size.

they are built to fit a rectangular lens. The lenses are kept in place by leaving a lip along the edge of one side of the cage mount and using set screws to keep the lenses from falling out. On the 130mm lens mount, a notch is cut out of the lip because the major axis of the beam would overlap with the lip.

2.2.2 Retroreflection

The lin $\perp$ lin configuration can be created by using two counterprogating independent beams or by reflecting and rotating the polarization of a single beam. We chose to use retroreflection to use optical power more efficiently. After the laser passes through the atomic beam, it is focused by a 2" diameter 75mm focal length lens to a point on a mirror 75 mm away. The beam profile will focus to a point on the mirror and reflect back to its incoming beam profile. To shift the polarization by 90°, a quarter wave plate is placed immediately before the mirror. As the incoming linearly polarized beam passes through the waveplate, it is converted to circularly polarized. After the beam is reflected, it will also be also circularly polarized, but in the opposite direction. After it passes through the waveplate, it will be linearly polarized, but orthogonal to the original incoming polarization.

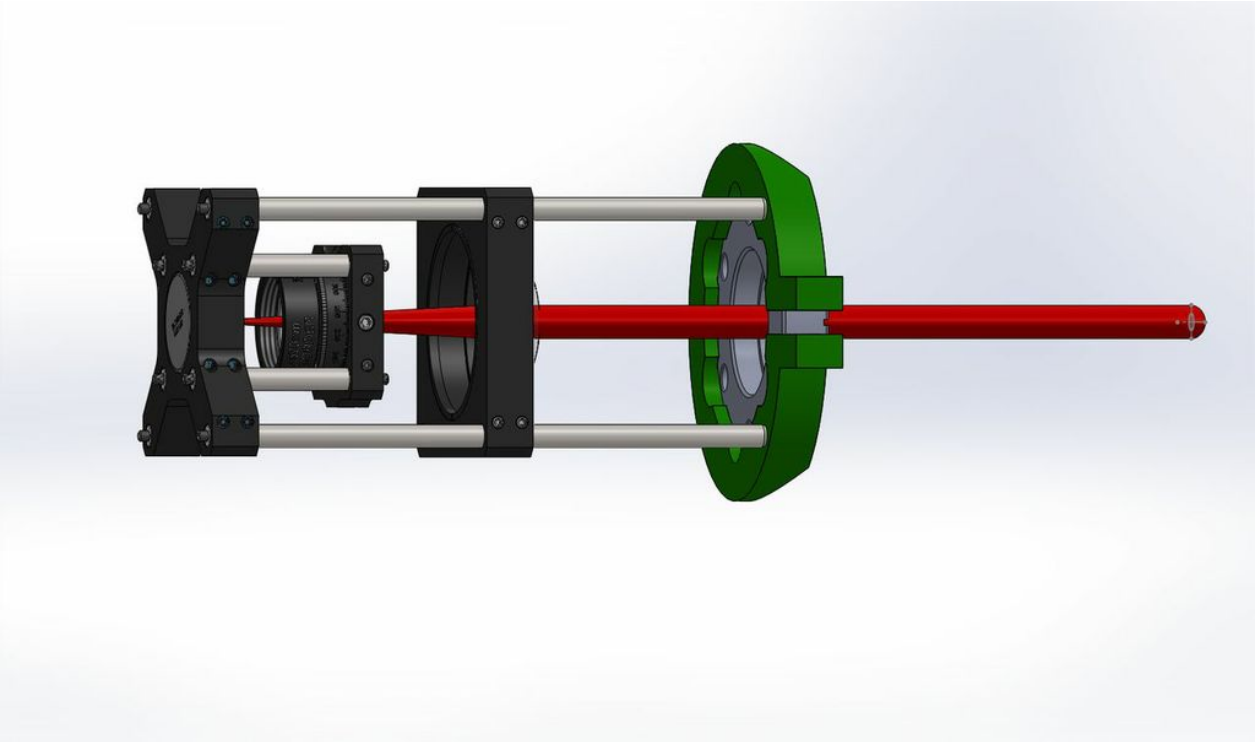

Figure 10: The light exits the atomic beam through a cage system similar to the one it entered the system. The light is focused by a 2" diameter, 75mm focal length lens to a point on a broadband dielectric mirror. The lens is mounted in a 60mm Thorlabs cage plate and the mirror inside an LCP02 cage plate. The quarter waveplate is mounted between the lens and mirror in a Thorlabs cage rotation mount attached to the system by means of a 30mm Thorlabs cage system.

2.3 Zeeman slower

After the first round of fast beam transverse cooling, the atomic beam will be well collimated, but with longitudinal speed too great to be trapped by a magneto-optical trap. A common tool used to slow a linear atomic beam to trappable velocities is a Zeeman slower. A Zeeman slower cools an atomic beam by using a counter-propagating laser beam with an applied spatially varying magnetic field. The beam is red detuned from the resonant frequency of the atomic transition. Zeeman slowers take advantage of the shift in the energy levels of an atomic transition in the presence of a magnetic field by using this shift to counteract the Doppler shift of the moving atoms.

2.3.1 Zeeman Effect

In addition to velocity and electric field, the energy between different atomic levels is also affected by the strength of the magnetic field and the relative direction of the electron's angular momentum. Assuming the magnetic field is small, it can be treated using perturbation theory. The energy of the perturbation will be the dot product of the magnetic field and the atomic magnetic moment in the direction of the magnetic field. The magnitude of the Zeeman shift will be

$$E_{Zeeman} = \mu_B B m_l g_j$$

where μ_B is the Bohr magneton, m_l is the angular momentum in the direction of the magnetic field and g_j is the atomic Lande g factor.[7] The atomic magnetic moment is defined by $\vec{\mu} =$ This Zeeman shift lifts the degeneracy of states that would otherwise have the same energy and shifts the difference in energy between two states with different m_l values.

Because the atomic beam is sufficiently narrow and isotropic, we assume that the magnetic field near the beam varies only along the axis of the beam. The easiest way to construct this magnetic field is with a solenoid with varying coil densities along its shared axis with the atomic beam.

When the atoms enter the Zeeman slower, they will be traveling with a mean velocity of several hundred meters per second, well outside the cooling regime of the counter-propagating laser in the absence of a magnetic field. In order to slow the fast moving beam, the counter-propagating laser beam must be near resonant with the atomic transition. Because the Doppler shift has changed the frequency of the light in the atom's frame, this can be acheived by setting the Zeeman shift due to the B field equal to the Doppler shift from the velocity of the atomic beam. For arbitrary velocity v,

$$\hbar\Delta\omega_{Zeeman} = \hbar\Delta\omega_{Doppler}$$

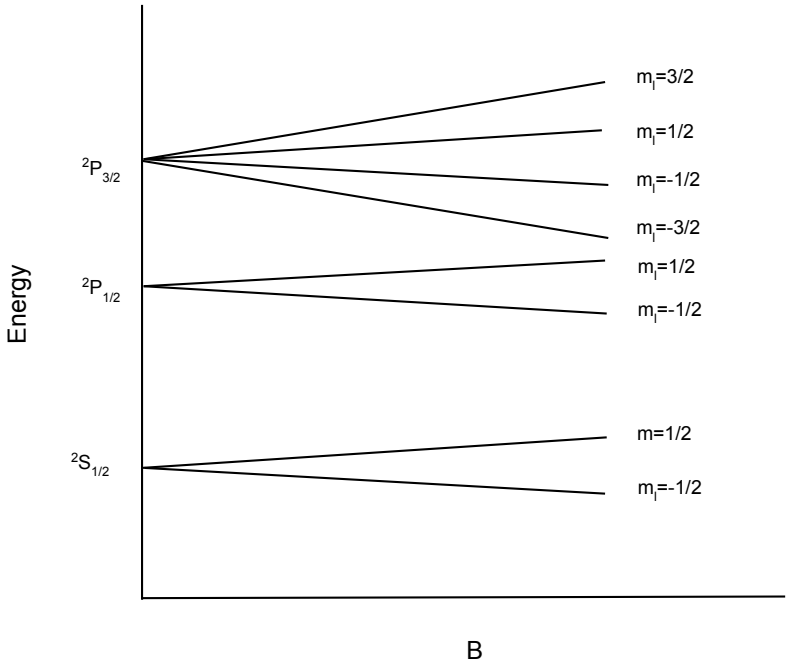

Figure 11: The energy of each state shifts as the magnetic field increases. This shift lifts the degeneracies of states with the same total angular momentum, but with differing angular momentum in the direction of the magnetic field. The slope of each line is proportional to m_l.

or

$$\mu_B B m_l g_j = \hbar \frac{v}{c} \omega_0$$

which implies that we should create a magnetic field

$$\vec{B} = \frac{\hbar v \omega_0}{c \mu m_l g_j}$$

If we assume a constant Doppler force and therefore constant acceleration $\vec{a} = \frac{d\vec{v}}{dt}$, the beam will travel with speed

$$v(z) = \sqrt{v_0^2 + 2az}$$

where we have defined the positive z axis to be along the direction of atomic beam propagation and the origin is the beginning of the Zeeman slower. Because B must be proportional to v,

$$B(z) = \sqrt{B_0^2 + 2\frac{F}{m} z}$$

Setting $B(Z) = 0$, where Z is the length of the Zeeman slower gives

$$F = \frac{-m B_0^2}{2Z}$$

The magnitude of the force is determined from the equation for force derived in section 1. The Zeeman effect shifts the resonant frequency in the same manner in which the Doppler effect shifts the resonant frequency.

$$\vec{F} = \frac{s_0 (\frac{\Gamma}{2})^3 \hbar \vec{k}}{(\delta - \vec{v} \cdot \vec{k} - \frac{\mu_B B m_l g_j}{\hbar})^2 + (s_0 + 1)(\frac{\Gamma}{2})^2} = \frac{-m B_0^2}{2Z} \hat{z}$$

$$B(z) = B_0 \sqrt{1 - \frac{z}{Z}}$$

The constant B_0 is determined by the length of the Zeeman slower as well as the Doppler force provided by the counter-propagating beam. This magnetic field can be created by building a solenoid with n turns per unit length where

$$B = \mu_0 n I$$

or

$$n = \frac{B}{\mu_0 I}$$

Either the density of the loops or the current in the loops must vary with position to create a spatially varying magnetic field. Our design uses few loops, but high current in the loops to create the necessary magnetic field. We used a hollow copper wire with square cross section with cold water pumped through the wire to act as a heat sink in order to prevent to the solenoid from overheating.

After passing through the Zeeman slower, the atomic speed will be reduced, however the beam will no longer be well collimated. The dispersion angle is the ratio of the transverse velocity of the beam to the the longitudinal velocity. Because the Zeeman slower decreased the longitudinal velocity of the beam from several hundred meters per second to tens of meters per second, the dispersion angle will increase inversely with the decrease of the longitudinal velocity. Also, because the beam has been subject to Doppler cooling in only one dimension, after each atomic cycle, the atom will emit a photon with momentum $\hbar\vec{k}$ and gain a corresponding momentum in the opposite direction with no mitigating forces in the transverse directions. Because the direction of emission is random, the expectation value of the transverse momentum will be zero, but the expection value of the square of the transverse momentum will increase with the number of momentum kicks,

$$< p_T^2 >= \frac{2}{3} N(\hbar k)^2$$

The factor of $\frac{2}{3}$ comes in because the transverse momentum consists of two of the three degrees of freedom.

The solid angle of the beam propagation will be too large for a sufficient number of atoms to load into to the magneto-optical trap, necessitating another round of transverse cooling.

2.4 Slow Beam Cooling Design

After the Zeeman slower, the longitudinal velocity is sufficiently low for the atoms to be trapped by the magneto-optical trap, but the solid angle of divergence is too large for most of the atoms to hit the trap. In order to collimate the atomic beam, we use another round of transverse cooling. The atomic beam passes through a 1.33" vaccuum cube with CF133 Flanges on each side. Because the beam is diverging over the course of the cube, it is beneficial to maximize the area of the incoming laser beams to maximize the number of atoms that interact with the transverse cooling beams. Because the windows of the CF flanges are circular, the incoming beams are also circular. This is simpler than the fast beam cooling because it only requires a single circular lens. We used a 75mm lens 75mm from the output of the fiber to collimate the beam. The $1/e^2$ diameter of the collimated beam will be $2NA * f = 16.5mm$, just less than the diameter of the window.

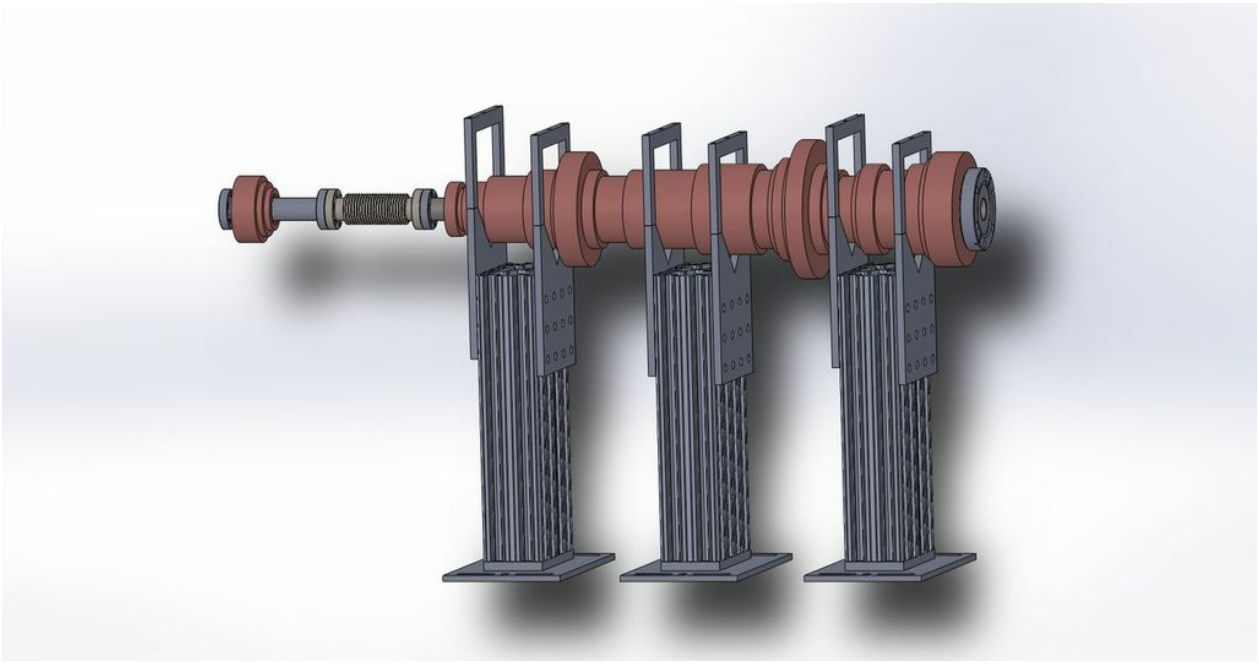

Figure 12: The 3 dimensional model of the Zeeman slower. The magnitude of the current and coil density varies along the z axis in order to create a B field $B(z) = B_0\sqrt{1-\frac{z}{Z}}$. Design Credit: Zach Geiger

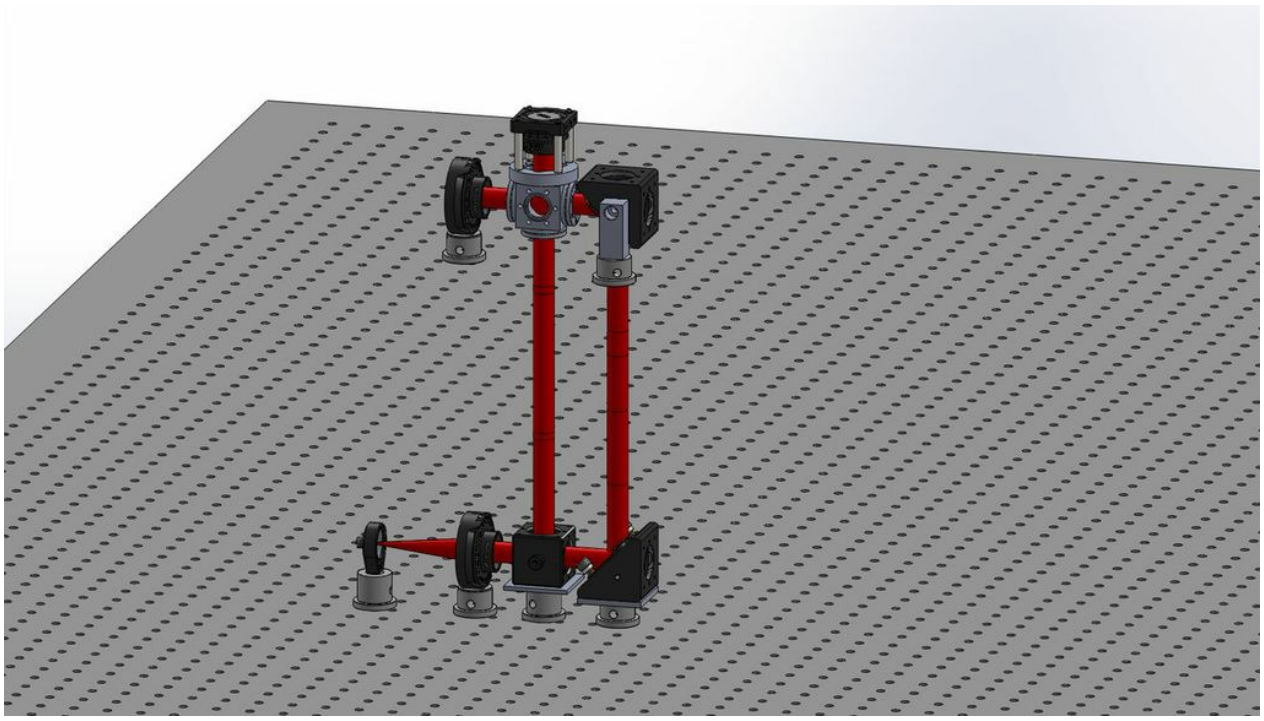

Figure 13: The three dimensional representation of the post Zeeman slower Transverse cooling. The optics closest to the atomic beam will be mounted on a small breadboard that has yet to be designed(not shown). The breadboard will have a hole to allow the laser beams to pass through.

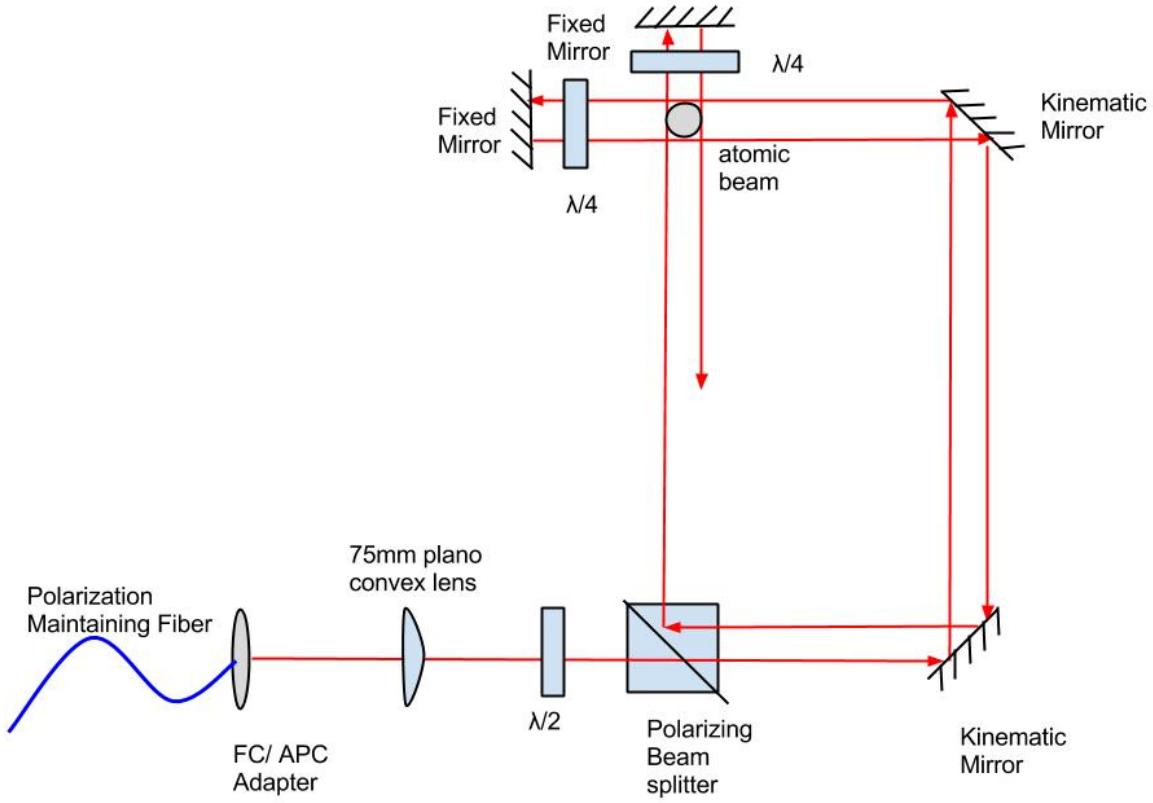

Figure 14: The schematic of the Post Zeeman slower Transverse Cooling. The light exits polarization maintaining fiber before being collimated by a 75mm lens. A half wave plate is used to polarize the light in the vertical direction so that it will pass through the polarizing beam splitter. It then reflects off of a kinematic mirror upwards through a small breadboard where a second kinematic mirror reflects the beam through the atomic beam. After passing through the atomic beam, the light passes through a quarter wave plate and is reflected by a mirror back through the quarter wave plate and atomic beam, but with orthogonal linear polarization. The beam is then diverted back to the lower optical table by the same kinematic mirrors used to bring it up. Now that its polarization is rotated 90°, it will be reflected by the beam splitter through the atomic beam. A quarter wave plate and mirror reflect the light back through the atomic beam.

2.4.1 Beam Path

Because the post Zeeman slower transverse cooling apparatus is attached to a small tube off of the vacuum main chamber, it cannot support the weight of four clamps attached to its sides. Because of this, most of the optics are placed on an optical table below the atomic beam. The beam exits from an FC/APC adapter and expands to the 75mm collimating lens. After collimating, the beam passes through a half wave plate to shift the polarization to vertical. The beam then passes through a polarizing beam splitter directly under the transverse cooling window with the reflection axis lying 45° from the vertical such that vertically polarized light is undeflected and horizontally polarized light is reflected down. After the light passes through the beam splitter, it is deflected by an elliptical mirror mounted 45° from vertical, perpendicular to the reflection plane of the beam splitting cube. The beam is directed vertically to a small breadboard below the vaccum chamber where it is deflected by another elliptical mirror mounted 45° from vertical, parallel to the reflection plane of the beam splitting cube. The beam is deflected by the mirror into the transverse cooling window. After passing through the window, the polarization of the beam is rotated and reflected by a quarter wave plate and mirror before passing back through the window and down the same optical path as the incoming beam until it reaches the beam splitting cube. Because the polarization of the beam is now rotated 90°, it will be reflected upwards by the beam splitting cube through the bottom transverse cooling window. After passing through the atomic beam, it is reflected and polarization shifted by a quarter waveplate and mirror clamped to the top window of the transverse cooling cube. After the beam is reflected, it passes back through the atomic beam and goes vertically through the beam splitting cube undeflected.

This arrangment allows one laser beam to pass through the atomic beam in two sets of counter-propagating directions.

2.4.2 Optomechanics

The atomic beam is several inches above the optical table holding the majority of the optics for the slow beam cooling. In order to transport the light from the optical table to the plane of the atomic beam, some cleverness must be used, especially in the orientation of the polarizing beam splitting cube and the kinematic mirror mounts. Neither the polarizing beam splitting cube nor the kinematic mirror mounts are designed to be mounted vertically. We designed and built plates with four 4-40 thru holes to couple to the backside of the each mount and a single 8-32 tapped hole to couple to a 3/4 inch pedestal pillar post. The thickness of the plates is cut such that the lens and waveplate are concentric with the beam splitter cube and with the projection of the elliptical mirror onto the plane orthogonal to the direction of the

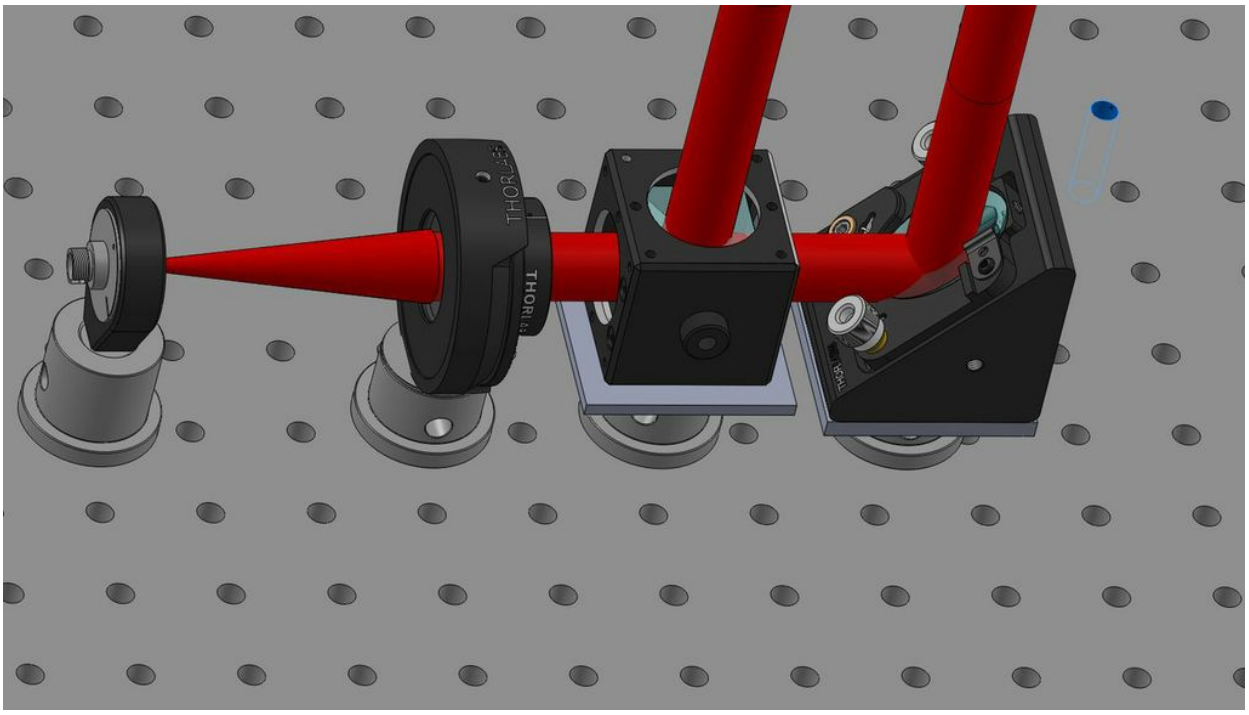

Figure 15: The three dimensional representation of the optics used for the post Zeeman slower transverse cooling mounted to the lower optical table. Machined aluminum plates are designed in order to ensure that the beam passes through the center of each optic, and to allow the optics to be mounted to Thorlabs pedestal pillar posts.

incoming beam.

3 Magneto-Optical Trapping

After the atoms pass through the two rounds of transverse cooling and Zeeman slower, they will be slow enough and sufficiently collimated to be trapped. They will enter the main chamber, which is under ultra high vacuum to reduce collisions with stray atoms. The atoms will travel toward the intersection of three sets of counter-propagating laser beams where they will be trapped and cooled by the laser beams and overlaying magnetic quadrupole field. The modular optics were designed by Erik Anciaux while the machine chamber was designed by Shankari Rajagopal and the magnetic quadrupole field was designed by Ruwan Senaratne and Shankari Rajagopal.

3.1 Theory

In the introduction, we outlined a process for which atoms can be cooled using three sets of counter-propagating laser beams. The atoms can be spatially confined using a spatially varying magnetic quadrupole field with zero point aligned at the center of the intersection

of the counter-propagating beams. To this point, we have made no assumptions of the polarization of the incoming beams. By cleverly orienting the polarization of light, we can use a polarization gradient to decrease the average energy of the atoms to the energy gained by emitting a single photon. Because the direction of the emitted photon is still random, polarization gradient cooling cannot decrease the momentum below $|\hbar\vec{k}|$. This corresponds to a lower energy limit of $E = k_b T_{Recoil} = \frac{|\hbar\vec{k}|^2}{2m}$ or $T_{Recoil} = \frac{|\hbar\vec{k}|^2}{2mk_b}$, which is typically an order of magnitude below the Doppler Limit. In order to further cool the atoms, we use evaporative cooling to leak the hottest atoms while keeping the coldest atoms, lowering the average energy of the atoms in the sample.

3.1.1 Magnetic Quadrupole Field

While optical molasses can effectively slow the atoms to the recoil limit, it cannot affect the position of the atoms. An atom, even with near zero velocity could escape from the trap. A position dependent magnetic field can be added to the laser array to make the optical force on the atoms position dependent. In a magneto-optical trap, a magnetic quadrupole field is arranged such that the intersection of the laser beams corresponds to the point of zero magnetic field. The quadrupole field is created by running opposite currents in two parallel circular loops of equal radius, separated by an orthogonal distance equal to the radius. This configuration of currents is known as the anti-Helmholtz configuration. Near the center of the two loops, the magnetic field will be proportional to

$$B \propto -x\hat{x} - y\hat{y} + 2z\hat{z}$$

close to the origin where the origin is defined to be the midpoint between the two coils along the central axis. The z-axis is defined to point from the center of one coil to the center of the other. [8]

As the distance from the center of the trap increases, the strength of the magnetic field increases. The magnetic field causes the resonant frequency of absorption to shift by

$$\Delta\omega = \frac{\vec{\mu} \cdot \vec{B}}{\hbar}$$

where $\vec{\mu}$ is the magnetic moment and $\vec{B}$ is the magnetic field. If atoms with near zero velocity stray far enough from the center of the trap, the magnetic field gradient will cause a large enough shift such that the incoming laser light is resonant with the atomic transition frequency and will provide a momentum kick towards the center of the trap.

Because the lasers provide a force opposite the velocity of the atoms and the magnetic field provides a force towards the intersection of the beams, the atoms will cool to the Doppler

limit and be confined near the center of the trap. This system is an analog to the three dimensional damped oscillator with force field

$$\vec{F} = -\alpha\vec{x} - \beta\vec{v}$$

where α and β are constants of proportionality. This cooling and trapping will increase the phase space density of the atoms because the temperature decreases to the recoil limit and the density increases as more atoms are loaded into the trap.

When an atom absorbs a photon, in addition to absorbing its energy and momentum, it will also absorb its angular momentum along the quantization axis. Absorbing a $\sigma+$ polarized photon will increase the atoms angular momenutm by $\hbar$ while absorbing a $\sigma-$ polarized photon will decrease the atoms angular momenutm by $\hbar$. Absorbing a linearly polarized photon will not change the angular momemtum of the atom. Similarly, when the atom emits a photon, if the emitted photon is $\sigma+$ polarized, the atomic angular momentum will decrease by $\hbar$ and if the photon is $\sigma-$ polarized, the atomic angular momentum will increase by $\hbar$. If the emitted photon is linearly polarized, it will not affect the atomic angular momentum.

If the magnetic field at the location of the atom is positive, then a σ^- polarized photon would excite the atom to a state to a state with less energy. Because the laser is detuned from resonance, σ^- light will be more likely to interact with atoms in locations with $B > 0$. If the magnetic field at the location of the atom is negative, then a σ^+ polarized photon would excite the atom to a state to a state with less energy and σ^+ light will be more likely to interact with atoms in locations with $B < 0$.

This discrepancy can be taken advantage of by using counter-propagating beams with opposite circular polarization with the σ^+ beam in the direction of increasing magnetic field and the σ^- beam in the direction of decreasing magnetic field. This arrangement, in conjuction with the position dependent magnetic field causes the laser beams to interact more with atoms on the same side of the origin as the source of the beam. The net result will be the laser beam applying a force that is proportional to the distance from the origin and toward the origin.

3.1.2 Polarization Gradient Cooling

If we use counter-propagating beams of opposite circular polarization, there will be a spatially varying electric field. Over the course of a wavelength, the total electric field vector will rotate. This polarization gradient will cause a split in the energy levels of the ground state due to the AC Stark Effect.[9] Any state may have higher energy depending on the location within the polarization gradient. [10]

Because the laser is red detuned, the laser will be more likely to excite atoms with energy

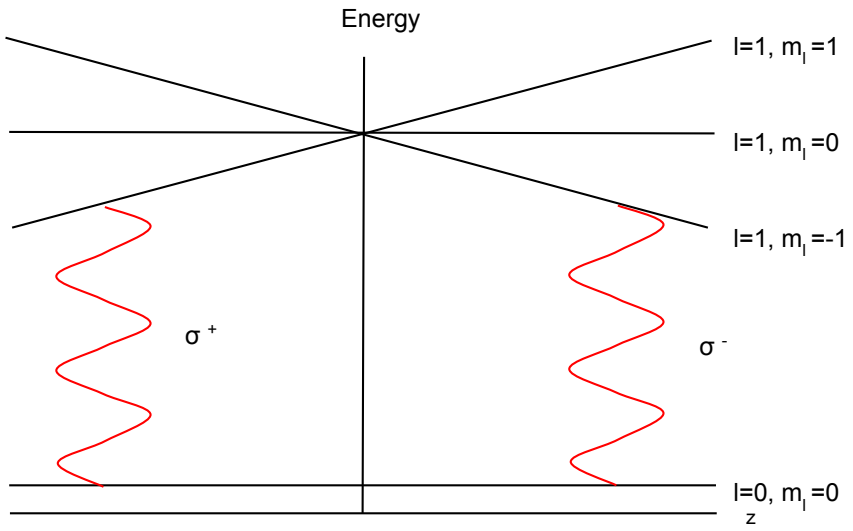

Figure 16: The magnetic field inceases with z. The ground state has no angular momentum, therefore the energy of the ground state does not change. The energy of the excited state with $m_l = 1$ increases with z and the energy of the excited state with $m_l = -1$ decreases with z. Atoms excited by a $\sigma+$ photon will be excited to the $m_l = 1$ state and atoms excited by a $\sigma-$ photon will be excited to the $m_l = -1$ state. Because the incoming light is red detuned, it will excite more atoms to the lower energy state. The $\sigma+$ beam is therefore oriented along the direction of increasing magnetic field in order to apply a net force to atoms where the magnetic field is less than zero and vice versa.

higher than the zero electric field ground state energy to compensate for the AC Stark shift, while it will not interact with atoms in states with energy less than that of the zero field ground state. An atom in the state with higher energy can be excited to an excited state by the incoming photon, but after emitting a photon can then decay either to the state of higher or lower energy. As an atom travels through the polarization gradient, it travels from a state with minimum potential energy and maximum kinetic energy to a state with maximum potential energy and minimum kinetic energy then absorbs and emits a photon and returns to the state of minimum potential energy, losing the difference between the maximum and minimum potential energies in the process. This cycle will repeat until the atom no longer has sufficient kinetic energy to reach the location of maximum potential energy for its state. The atoms will only lose energy because because they begin each cycle in a higher energy ground state, then can end the cycle in the same energy state or in a state with lower energy. Over a complete cycle, the atoms cannot transfer from a state with lower energy to a state with higher energy because the red detuned laser will not excite atoms in a lower energy state. This process is referred to as Sisyphus cooling, after Sisyphus in Greek Mythology. According to legend, Sisyphus would push a heavy rock from the bottom of a valley to the top of a hill, only to have the rock immediately roll back down to the bottom of the valley.[11] Because Sisyphus cooling can take advantage of energy levels splitting due to the polarization gradient, it can lower the temperature beyond the Doppler limit. Sisyphus cooling changes the momentum of an atom by a discrete step $\hbar\vec{k}$ for each step. Because the direction of the emitted photon is still random, Sisyphus Cooling cannot decrease the expectation value of the momentum below $|\hbar\vec{k}|$, or cannot decrease the temperature below $T_{Recoil} = \frac{|\hbar\vec{k}|^2}{2mk_b}$. The recoil limit is on the order of one microKelvin.

3.1.3 Evaporative Cooling

After the atoms are cooled to the recoil limit, they can be further cooled using evaporation. Evaporative cooling takes advantage of the Maxwell Boltzmann distribution of atomic speeds. The trap is designed such that the lower velocity atoms are kept in the trap, but the higher velocity atoms are leaked out. After the higher velocity atoms escape, the existing atoms rethermalize into a Maxwell Boltzmann distribution, but with a lower energy and therefore a lower temperature. This process is repeated many times, each time losing only a small number of atoms and decreasing in temperature by a small amount. This technique is used to decrease the temperatures of an atomic gas below the recoil limit to the temperatures needed for the atoms to form a Bose-Einstein condensate or degenerate Fermi gas.[12]

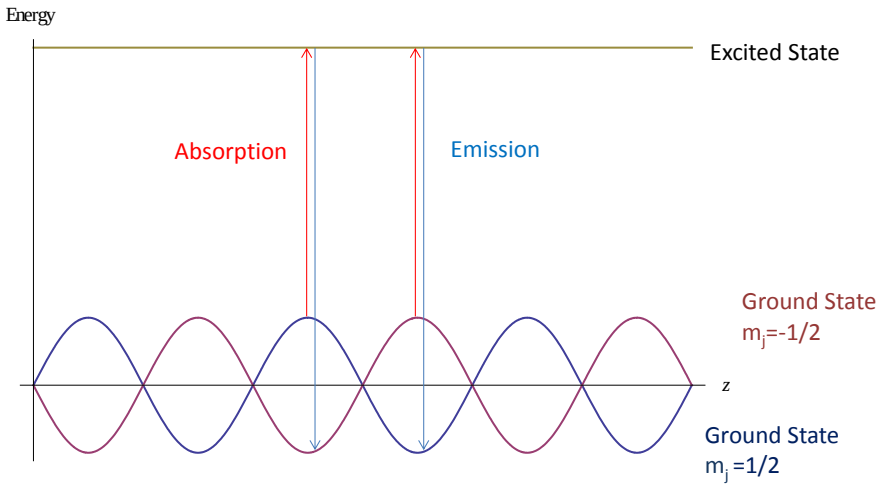

Figure 17: As an atom in the ground state travels through a polarization gradient, its energy will shift due to the AC Stark effect. When it travels through the gradient to a state with maximum energy, it will absorb a photon and become excited to to the excited state. The atom will then emit the photon and return to either the original higher energy state or to the opposite, lower energy state. If it returns to the lower energy ground state, the atom will lose an energy equal to the difference in energy between the two ground states. Conservation of energy is not violated because the emitted photon has a higher frequency and therefore higher energy than the absorbed photon.

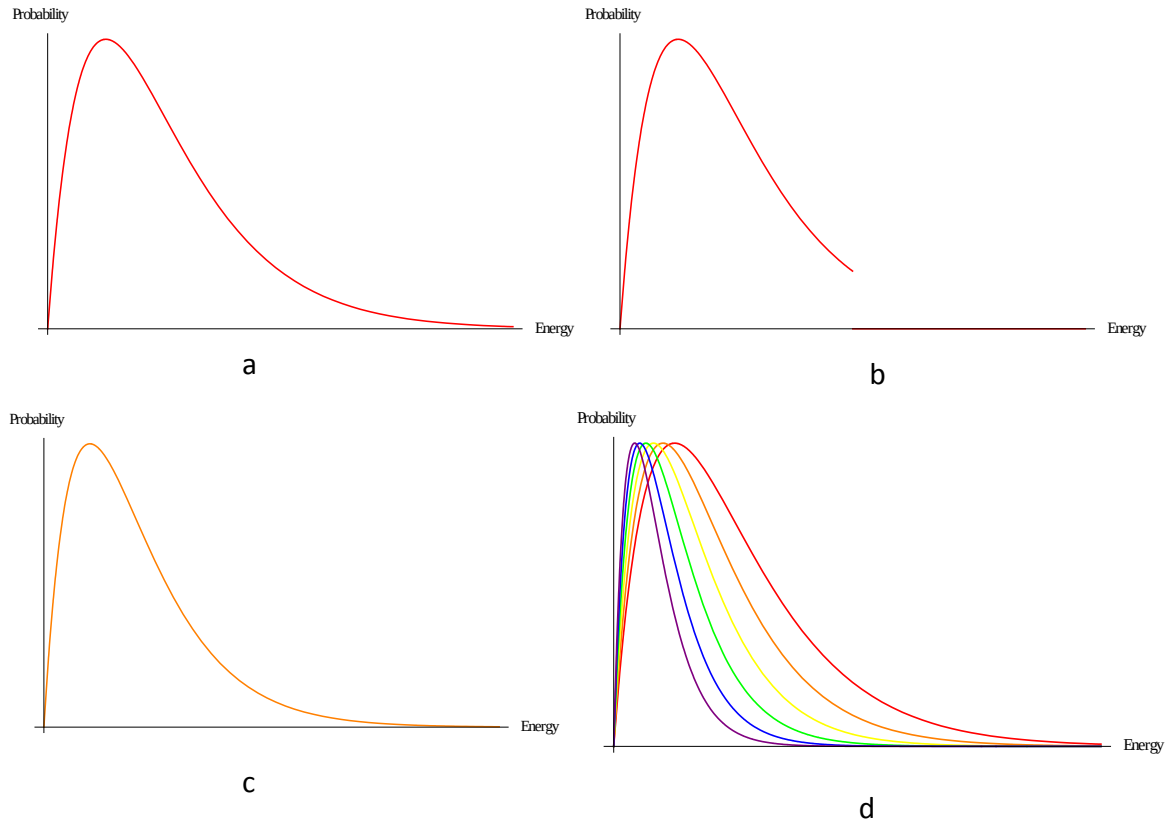

Figure 18: The cycle of evaporative cooling. a) The distribution of atomic kinetic energy before evaporative cooling. b) The highest energy atoms are removed. c) The distribution rethermalizes with a lower average enregy. d) If the initial distribution starts in a state modeled by the red curve, after successive cycles of evaporative cooling, the distribution will shift through states modeled by the orange, yellow, green, blue and purple states. This cycle can be repeated indefinitely until the desired average energy is reached, however the number of atoms in the trap will also decrease. In order to maximize the number of atoms while minimizing the temperature, the highest energy atoms must be released adiabatically.

3.2 Magneto-Optical Trap Modular Optics

The magneto-optical trap requires three sets of counter-propagating beams, for a total of six incoming beams. In order for the equilibrium force on stationary atoms in the trap to be zero, the power of each beam must be nearly equal. Also, in order to interact with every atom in the trap, the beam must be wider than the incoming atomic beam. For each set of counter-propagating beams, one must be left circularly polarized and the other must be right circularly polarized. For our experiment, this requires six beams of equal power, one inch in diameter, three of which are left circularly polarized and three of which are right circularly polarized.

3.2.1 Fiber Splitting

The six beams of equal power are manufactured by inputting two beams of light into the inputs of a 2x6 FC/APC non-polarization maintaining fiber splitter. The second input beam is for a repumper laser, which will not be discussed here. The specific fiber splitter we used was purchased from OZ Optics. The fiber is designed to output the incoming light from the two inputs equally among the six outputs. The exact values of the outgoing power vary between 14 and 19 percent of the input power. This discrepancy can be mitigated by pairing the two lowest power beams, the two middle power beams and two highest power beams into pairs of counter-propagating beams. This minimizes the difference in power between the two counter-propagating beams. The uniformity of the power across all beams is not as vital as the uniformity of the power between two counter-propagating beams.

In this experiment, we used non-polarization maintaining fiber as opposed to polarization maintining fiber. If a linearly polarized beam enters the fiber, a linearly polarized beam will exit the fiber, however the direction of the polarization will depend on the orientation of the fiber. If the fiber is moved at any point between input and output, the polarization of the output beam will rotate. This can be rectified by keeping the fiber completely still during the experiment. The polarization of the outcoming beam can then be shifted to the desired angle by placing a half wave plate after the output of the fiber, or can be made circular by placing a quarter wave plate after the output of the fiber with fast axis rotated 45° from the polarization of the light.

3.2.2 Optomechanics

Each fiber ouptut is converted to free space optics by coupling the fiber output to a Thorlabs FC/APC fiber collimation package. The collimation package is mounted to a cage system by means of a collimation package adapter inside a cage plate. The collimation package will collimate the beam with a $\frac{1}{e^2}$ diameter of 4.5mm. The beam will then go through a

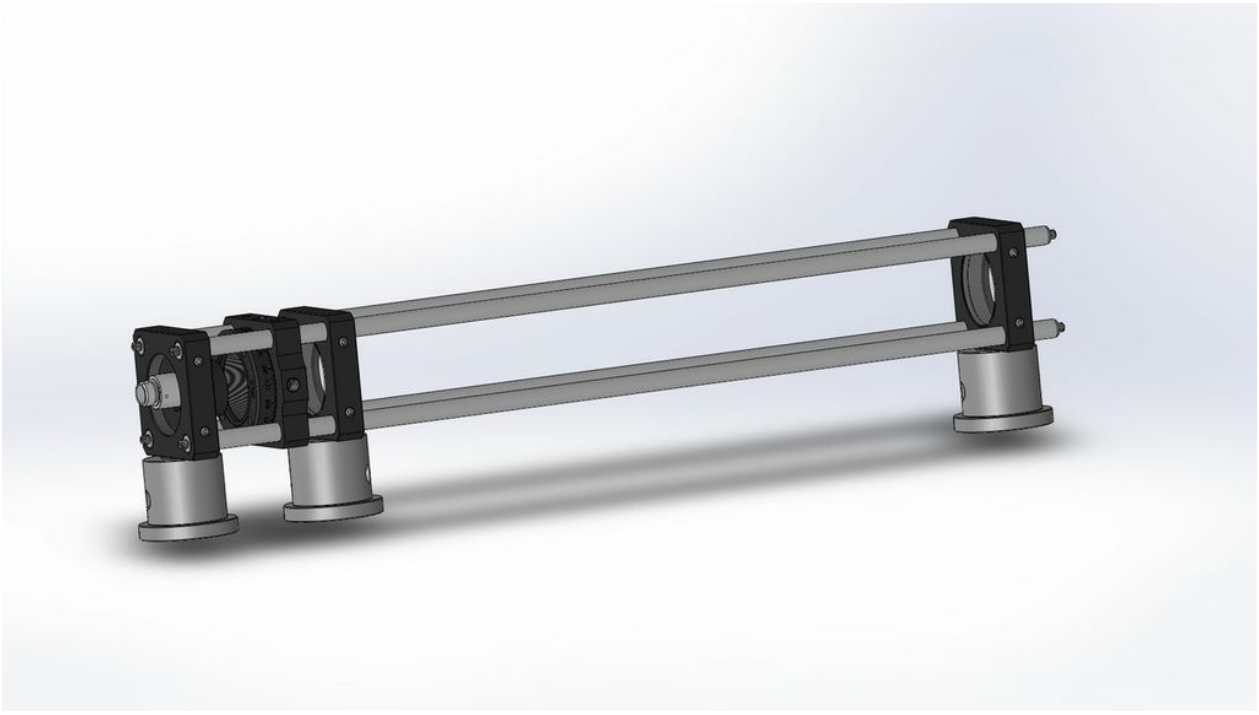

Figure 19: This is the three dimensional representation of the magneto-optical trap modular optics. The light enters through an FC/APC fiber collimation package at the left, travels through a quarter waveplate inside a cage rotation mount, followed by a telescope. The first lens of the telescope has focal length 35mm while the second has focal length 200mm.

quarter wave plate mounted inside a cage rotation mount. The fast axis of the rotation mount should be oriented 45° from the direction of polarization in order to create circularly polarized light. The waveplate should be oriented 45° counterclockwise to create left handed circularly polarized light or 45° clockwise to create right circularly polarized light.

After the beam is circularly polarized, it passes through a cage mounted telescope with initial lens focal length 35mm and final lens focal length 200mm. This expands the beam diameter from 4.5mm to 25.4mm.

3.3 Movable Mirror Apparatus

The six magneto-optical trap beams are diverted from the cage systems toward six windows of the vacuum chamber. After the atoms are cooled to ultracold temperatures, optical lattice beams will be aimed through the same windows to manipulate the cold atoms. In order to control whether the magneto-optical trap beams pass through the windows or the lattice beams pass through the windows, there must be a mechanism to switch between the beams. We designed and built a solenoid valve activated moveable mirror that could be raised or lowered by turning the solenoid valves on or off.

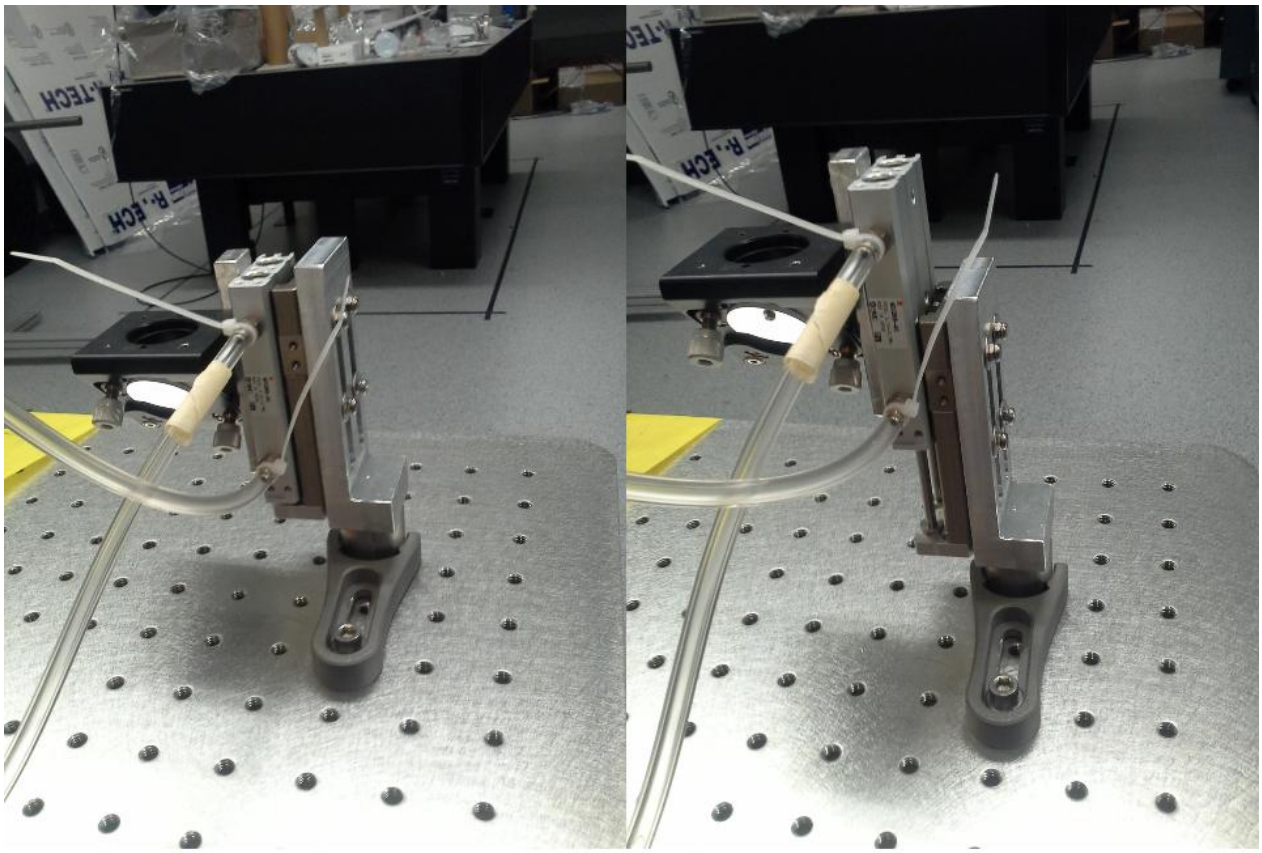

Figure 20: The movable mirror in the depressed(left) and elevated(right) positions. Pressure applied to the lower tube will depress the mirror while pressure applied to the upper tube will elevate the mirror.

3.3.1 Mirror Mounting

We mounted a Thorlabs kinematic 45° turning mirror to an SMC slide table, part number MXQR8-40, using a machined 3" by .5" by .3" block with two counterbored through holes on one side to mount to the slide table and a single through hole on the opposite side to mount to the mirror mount. On the opposite face of the slide table, we machined an L shaped mount with straight slots along the long side to allow for a continuum of heights for which to mount the stage to the L mount. On the bottom of an L mount is an 8-32 threaded hole which can be used to attach the mounting apparatus to a Thorlabs pedestal pillar post, to be placed on an optical table.

3.3.2 Pneumatics

On the slide table are two threaded holes connecting two air chambers to the atmosphere. We inserted screw to hose barb adapters into the threaded holes and attached Tygon tubing

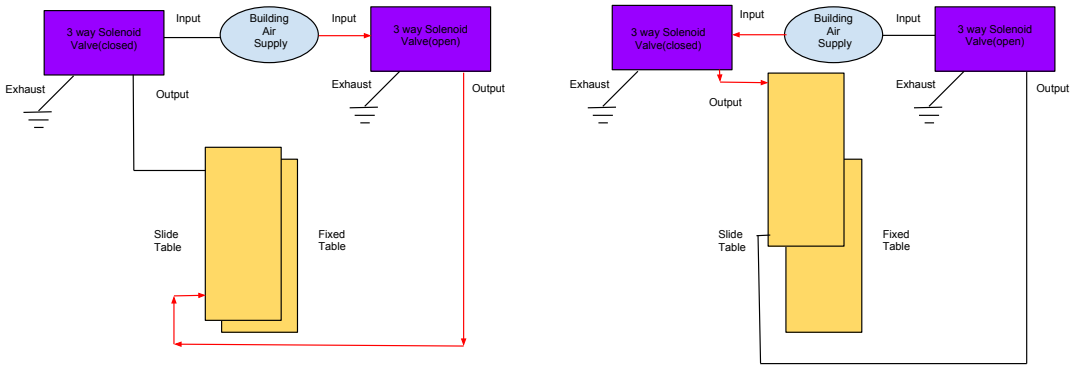

Figure 21: The schematic for the moveable mirror mount pneumatics with presssure applied to the bottom input of the slide table for the depressed state(left) and to the top input of the slide table for the elevated state(right)

to the barbs. The opposite end of the Tygon tubes were connected to the output of two 3 way STC solenoid valves. We connected the input of the valves to the building air supply to provide pressure to the air chambers. The exhaust outputs of the valves were left open to release air from the chamber when the valves were closed. We used a switch to open one valve while closing the other. The speed of the transition from the elevated state to the depressed state was controlled using a needle valve on the Tygon tubing. This prevents hard collisions between the moving parts of the slide table, ensuring that the mounted mirror remains in the same position over the course of many cycles.

4 Lithium

To this point, this thesis has covered general procedures of magneto-optical trapping without reference to the trapped atom. Our experiment will trap and cool neutral lithium atoms, of both ^{6}Li and ^{7}Li. Like all alkali metals, lithium is a solid at room temperature. In order to trap and cool individual atoms of lithium, the solid structure of the lithium must be broken so that individual lithium atoms can travel through the transverse cooling apparatuses and the Zeeman slower towards the trap. The Lithium sample is heated in an oven to 450° C, at which point it will have a vapor pressure on the order of 10^{19} atoms/m^3 and average atomic speed 1600 m/s. A nozzle will be placed at the edge of the oven to collimate the fast atoms toward the trap.

4.1 Isotopes

Lithium exists naturally in two different isotopes, ^{6}Li and ^{7}Li. In nature, about 92% of lithium atoms are ^{7}Li and the remaining 8% of atoms are ^{6}Li. ^{6}Li consists of three protons

and three neutrons in the nucleus and three electrons outside the nucleus, while ^{7}Li consists of three protons and four neutrons in the nucleus and three electrons outside the nucleus. Because electrons and and nucleons are all spin $\frac{1}{2}$ fermions, a particle composed of nucleons and electrons will have integer spin if the total number of constituent fermions is even and will have half integer spin if the total number of constituent fermions is odd. ^{6}Li has nine constituent fermions and will therefore be a composite fermion. ^{7}Li has ten constituent fermions and will therefore be a composite boson. Because ^{7}Li atoms are bosons, they readily Bose condense. ^{6}Li atoms on the other hand will form a degenerate Fermi gas. ^{6}Li nuclei have nuclear spin $I = 1$ and ^{7}Li nuclei have nuclear spin $I = \frac{3}{2}$.[13]

4.2 Electronic Structure

The first two electrons fill the $n = 1$ orbital and do not interact with the valence electron. The ground state of the atom will have the valence electron in the $n = 2$, $l = 0$ state. There are two possible electronic configuration with $n = 2$, $l = 0$, one with spin up, and one with spin down. Without considering hyperfine structure, the two states have equal energy. Hyperfine structure arises from the electron total angular momentum, $\vec{J} = \vec{L} + \vec{S}$ coupling with the nuclear spin and is proportional to their dot product, $\vec{J}.\vec{I}$. Because the orbital angular momentum $\vec{L}$ is zero, $J = S = \frac{1}{2}$. The dot product is solved by using the total atomic angular momentum quantum number $\vec{F}$.

$$\vec{F} = \vec{J} + \vec{I}$$

Squaring this relation gives,

$$F^2 = J^2 + I^2 + 2\vec{J} \cdot \vec{I}.$$

Rearranging terms gives

$$\vec{J}.\vec{I} = \frac{1}{2}(F^2 - J^2 - I^2)$$

[14] Because F^2, $J^2$and I^2 are operators with eigenvalues $F(F+1), J(J+1), I(I+1)$ respectively, the numerical value of $\vec{J} \cdot \vec{I}$ is given by

$$\frac{1}{2}(F(F+1) - J(J+1) - I(I+1)$$

For ^{6}Li, inserting $I = 1$ and $J = \frac{1}{2}$ gives

$$\vec{J} \cdot \vec{I} = \frac{1}{2}(F(F+1) - \frac{1}{2}(\frac{3}{2}) - (2)) = \frac{1}{2}(F(F+1) - \frac{11}{4})$$

For ^{7}Li, inserting $I = \frac{3}{2}$ and $J = \frac{1}{2}$ gives

$$\vec{J} \cdot \vec{I} = \frac{1}{2}(F(F+1) - \frac{1}{2}(\frac{3}{2}) - \frac{3}{2}(\frac{5}{2})) = \frac{1}{2}(F(F+1) - \frac{19}{4})$$

Because F is the sum of two angular momentum vectors, it can only take a value between their sum and the absolute value of their difference and must differ from both by an integer.

$$|I - J| \leq F \leq I + J$$

For ^{6}Li,

$$\frac{1}{2} \leq F \leq \frac{3}{2}$$

For ^{7}Li,

$$1 \leq F \leq 2$$

Therefore the only two values for F are $\frac{1}{2}$and $\frac{3}{2}$ for ^{6}Li, and 1 and 2 for ^{7}Li. Inserting these values back into our equation for $\vec{J} \cdot \vec{I}$ for ^{6}Li gives

$$\vec{J} \cdot \vec{I}|_{F=\frac{1}{2}} = \frac{1}{2}(\frac{1}{2}(\frac{3}{2}) - \frac{11}{4}) = -1$$

$$\vec{J} \cdot \vec{I}|_{F=\frac{3}{2}} = \frac{1}{2}(\frac{3}{2}(\frac{5}{2}) - \frac{11}{4}) = \frac{1}{2}$$

and for ^{7}Li,

$$\vec{J} \cdot \vec{I}|_{F=1} = \frac{1}{2}((2) - \frac{11}{4}) = -\frac{3}{8}$$

$$\vec{J} \cdot \vec{I}|_{F=2} = \frac{1}{2}(2(3) - \frac{11}{4}) = \frac{13}{8}$$

The constant of proportionality between the frequency and $\vec{J} \cdot \vec{I}$ is 152.1 MHz for^{6}Li and for 401.7 MHz ^{7}Li, therefore the $F = \frac{1}{2}$ is shifted by -152.1 MHz and the $F = \frac{3}{2}$ state is shifted by 76.0 MHz. Because the $F = \frac{1}{2}$ state is shfited to a state of lower energy, it is the ground state. For ^{7}Li, the $F = 1$ state is shifted by -150.6 MHz and the $F = 2$ is shifted by 652.8 MHz, therefore the $F = 1$ is the ground state.[13, 15]

4.2.1 Excited states

The lowest excited states not considering fine structure are the $^2P_{\frac{1}{2}}$ state and $^2P_{\frac{3}{2}}$ state. Each state consists of a single valence electron with spin $s = \frac{1}{2}$ and orbital angular momentum

$l = 1$. The ${}^2P_{\frac{1}{2}}$ state has total angular momentum $J = \frac{1}{2}$ and the ${}^2P_{\frac{3}{2}}$ state has total angular momentum $J = \frac{3}{2}$. The difference in energy between these two state arises due to spin orbit coupling. Spin orbit coupling arises due to the electronic spin interaction with the magnetic field of the electron's orbit. The interaction is proportional to the dot product of the orbital angular momentum L and electronic spin S.

$$E_{SOC} \propto \vec{L} \cdot \vec{S}$$

This dot product can be solved by using the total electronic angular momentum quantum number J.

$$\vec{J} = \vec{L} + \vec{S}$$

Squaring both sides gives

$$J^2 = L^2 + S^2 + 2\vec{L} \cdot \vec{S}$$

Rearranging terms gives

$$\vec{L}.\vec{S} = \frac{1}{2}(J^2 - L^2 - S^2)$$

The J^2, L^2 and S^2 operators have eigenvalues $J(J+1)$, $L(L+1)$ and $S(S+1)$ respectively.

$$E_{SOC} \propto \frac{1}{2}(J(J+1) - L(L+1) - S(S+1))$$

For ${}^2P_{\frac{1}{2}}$, $J = \frac{1}{2}$, $L = 1$, $S = \frac{1}{2}$

$$E_{SOC} \propto \frac{1}{2}(\frac{1}{2} * \frac{3}{2} - 1 * 2 - \frac{1}{2} * \frac{3}{2}) = \frac{1}{2}(\frac{3}{4} - 2 - \frac{3}{4}) = -1$$

For ${}^2P_{\frac{3}{2}}$, $J = \frac{3}{2}$, $L = 1$, $S = \frac{1}{2}$

$$E_{SOC} \propto \frac{1}{2}(\frac{3}{2} * \frac{5}{2} - 1 * 2 - \frac{1}{2} * \frac{3}{2}) = \frac{1}{2}(\frac{15}{4} - 2 - \frac{3}{4}) = \frac{1}{2}$$

Therefore, the ${}^2P_{\frac{3}{2}}$state has higher energy than the ${}^2P_{\frac{1}{2}}$ state. The constant of proportionality between the energy and $\hat{L} \cdot \vec{S}$ is $6.7GHz * h$. Therefore the the ${}^2P_{\frac{1}{2}}$ and ${}^2P_{\frac{3}{2}}$ are separated by 10.05 GHz. While the values of the energy between the ${}^2P_{\frac{3}{2}}$state and ${}^2P_{\frac{1}{2}}$ state differ slightly for ^{6}Li and ^{7}Li, they are identical to four significant figures.[15]

The energies for the hyperfine splitting for the $l = 1$ states can be determined by the method

used in Section 4.2. For ^{6}Li, in the $^2P_{\frac{1}{2}}$ state, F can take on values in the range

$$|J - I| \leq F \leq J + I$$

or

$$\frac{1}{2} \leq F \leq \frac{3}{2}$$

decreasing in integral increments from $J + I$. This gives $\frac{1}{2}$ and $\frac{3}{2}$ as the possible values of F. The hyperfine splitting of this state is proportional to

$$\vec{J} \cdot \vec{I} = \frac{1}{2}(F(F+1) - J(J+1) - I(I+1))$$

$$\vec{J} \cdot \vec{I}|_{F=\frac{1}{2}} = \frac{1}{2}(\frac{1}{2}(\frac{3}{2}) - \frac{1}{2}(\frac{3}{2}) - (2)) = \frac{1}{2}(\frac{3}{4} - \frac{3}{4} - 2) = -1$$

$$\vec{J} \cdot \vec{I}|_{F=\frac{3}{2}} = \frac{1}{2}(\frac{3}{2}(\frac{5}{2}) - \frac{1}{2}(\frac{3}{2}) - (2)) = \frac{1}{2}(\frac{15}{4} - \frac{3}{4} - 2) = \frac{1}{2}$$

For the $^2P_{\frac{3}{2}}$ state of ^{6}Li, the possible values of F are $\frac{5}{2}$, $\frac{3}{2}$ and$\frac{1}{2}$.

$$\vec{J} \cdot \vec{I}|_{F=\frac{1}{2}} = \frac{1}{2}(\frac{1}{2}(\frac{3}{2}) - \frac{3}{2}(\frac{5}{2}) - (2)) = \frac{1}{2}(\frac{3}{4} - \frac{15}{4} - 2) = -\frac{5}{2}$$

$$\vec{J} \cdot \vec{I}|_{F=\frac{3}{2}} = \frac{1}{2}(\frac{3}{2}(\frac{5}{2}) - \frac{3}{2}(\frac{5}{2}) - (2)) = \frac{1}{2}(\frac{15}{4} - \frac{15}{4} - 2) = -1$$

$$\vec{J} \cdot \vec{I}|_{F=\frac{5}{2}} = \frac{1}{2}(\frac{5}{2}(\frac{7}{2}) - \frac{3}{2}(\frac{5}{2}) - (2)) = \frac{1}{2}(\frac{35}{4} - \frac{15}{4} - 2) = \frac{3}{2}$$

The constant of proportionality for the $^2P_{\frac{1}{2}}$ is 17.4 MHz and -1.1 MHz for $^2P_{\frac{3}{2}}$. The negative constant of proportionality for the $^2P_{\frac{3}{2}}$ state implies that The $F = \frac{1}{2}$ state has the highest energy followed by the $F = \frac{3}{2}$state and then by the $F = \frac{5}{2}$ state. The hyperfine splitting between the $F = \frac{1}{2}$ line and $F = \frac{3}{2}$ line for the $^2P_{\frac{1}{2}}$ is

$$f_{HF} = (\frac{1}{2} -^{-} 1) * 17.4MHz = 26.1MHz$$

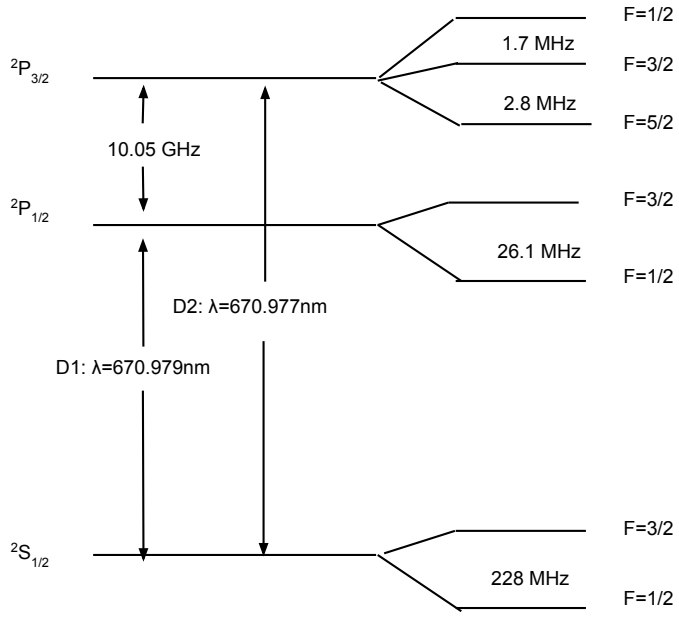

Figure 22: This chart shows the transition energies between states of Lithium 6[15]

The hyperfine splitting between the $F = \frac{1}{2}$ line and $F = \frac{3}{2}$ line for the $^2P_{\frac{3}{2}}$ is

$$f_{HF} = (^-\frac{5}{2} -^- 1) * -1.1MHz = 1.7MHz$$

and between the $F = \frac{3}{2}$ and $F = \frac{5}{2}$ line is

$$f_{HF} = (^-1 - \frac{3}{2}) * -1.1MHz = 2.8MHz$$

[?]

In ^{7}Li, the two $n = 2, l = 1$ states are also the $^2P_{\frac{1}{2}}$ state and the $^2P_{\frac{3}{2}}$ state, however the spin of the nucleus is $I = \frac{3}{2}$. For the $^2P_{\frac{1}{2}}$ state, F can take on values 1 or 2. For the $^2P_{\frac{3}{2}}$ state, F can take on the values 0, 1, 2, 3. The hyperfine splitting of the $^2P_{\frac{1}{2}}$ state is proportional to

$$\vec{J} \cdot \vec{I}|_{F=1} = \frac{1}{2}(1 * (2) - \frac{1}{2}(\frac{3}{2}) - \frac{3}{2}(\frac{5}{2})) = \frac{1}{2}(-\frac{5}{2}) = -\frac{5}{4}$$

$$\vec{J}\cdot\vec{I}|_{F=2} = \frac{1}{2}(2*(3) - \frac{1}{2}(\frac{3}{2}) - \frac{3}{2}(\frac{5}{2})) = \frac{1}{2}(\frac{3}{2}) = \frac{3}{4}$$

The constant of proportionality is 40.9MHz, giving a hyperfine splitting between the two states of

$$f_{HF} = (\frac{3}{4} -^{-} \frac{5}{4}) * 40.9MHz = 91.8MHz$$

The hyperfine splitting of the $^2P_{\frac{3}{2}}$ state is proportional to

$$\vec{J}\cdot\vec{I}|_{F=0} = \frac{1}{2}(-\frac{3}{2}(\frac{5}{2}) - \frac{3}{2}(\frac{5}{2})) = \frac{1}{2}(-\frac{15}{2}) = -\frac{15}{4}$$

$$\vec{J}\cdot\vec{I}|_{F=1} = \frac{1}{2}(1*(2) - \frac{3}{2}(\frac{5}{2}) - \frac{3}{2}(\frac{5}{2})) = \frac{1}{2}(-\frac{11}{2}) = -\frac{11}{4}$$

$$\vec{J}\cdot\vec{I}|_{F=2} = \frac{1}{2}(2*(3) - \frac{3}{2}(\frac{5}{2}) - \frac{3}{2}(\frac{5}{2})) = \frac{1}{2}(-\frac{3}{2}) = -\frac{3}{4}$$

$$\vec{J}\cdot\vec{I}|_{F=1} = \frac{1}{2}(3*(4) - \frac{3}{2}(\frac{5}{2}) - \frac{3}{2}(\frac{5}{2})) = \frac{1}{2}(\frac{9}{2}) = \frac{9}{4}$$

The constant of proportionality is -3.1MHz giving a hyperfine splitting between the $F = 0$ and $F = 1$ states

$$f_{HF} = -3.1(^{-}\frac{15}{4} - \frac{11}{4}) = 3.1MHz$$

and between the $F = 1$ and $F = 2$ states

$$f_{HF} = -3.1(^{-}\frac{11}{4} -^{-} \frac{3}{4}) = 6.2MHz$$

and between the $F = 2$ and $F = 3$ states

$$f_{HF} = -3.1(^{-}\frac{3}{4} - \frac{9}{4}) = 9.2MHz$$

The hyperfine states of the $^2P_{\frac{3}{2}}$ states of the both ^{6}Li and ^{7}Li are separated by less than the natural linewidth of the atomic transition and are therefore unresolved.[13]

4.3 Atomic Transitions

At any point, the vast majority of atoms in the atomic Lithium cloud will be in the ground

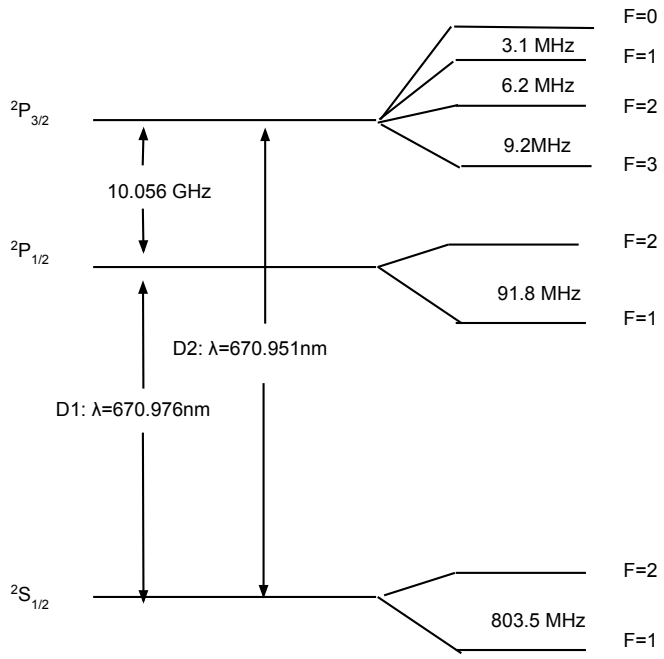

Figure 23: This chart shows the transition energies between states of Lithium 7[13]

state, ${}^2S_{\frac{1}{2}}$. This state has no orbital angular momentum, and the only contribution to the total angular momentum is the spin of the single valence electron. ^{6}Li and ^{7}Li have the same atomic states, neglecting hyperfine structure, however the energy spacing between the states differs depending on the isotope. The D1 line specifies the transition between the ${}^2S_{\frac{1}{2}}$ state and the ${}^2P_{\frac{1}{2}}$ state while the D2 line specifies the transition between the ${}^2S_{\frac{1}{2}}$ state and the ${}^2P_{\frac{3}{2}}$ state. For ^{6}Li, The D1 line corresponds to the energy of a photon of wavelength$\lambda = 670.979nm$ and the D2 line corresponds to the energy of a photon of wavelength $\lambda = 670.977nm$. For ^{7}Li, the D1 line corresponds to the energy of a photon of wavelength $\lambda = 670.976nm$ and the D2 line corresponds to the energy of a photon of wavelength $\lambda = 670.951nm$. [13]

4.3.1 Selection Rules

Each state with a given value of F can have $2F + 1$ possible hyperfine states. The states correspond to the total atomic angular momentum along the quantization axis.

$$m_F = F, F-1, ..., -F+1, -F$$

When a photon is absorbed by an atom in the ground state, the atom will be excited to the state with an energy higher than that of the ground state by the energy of the incoming

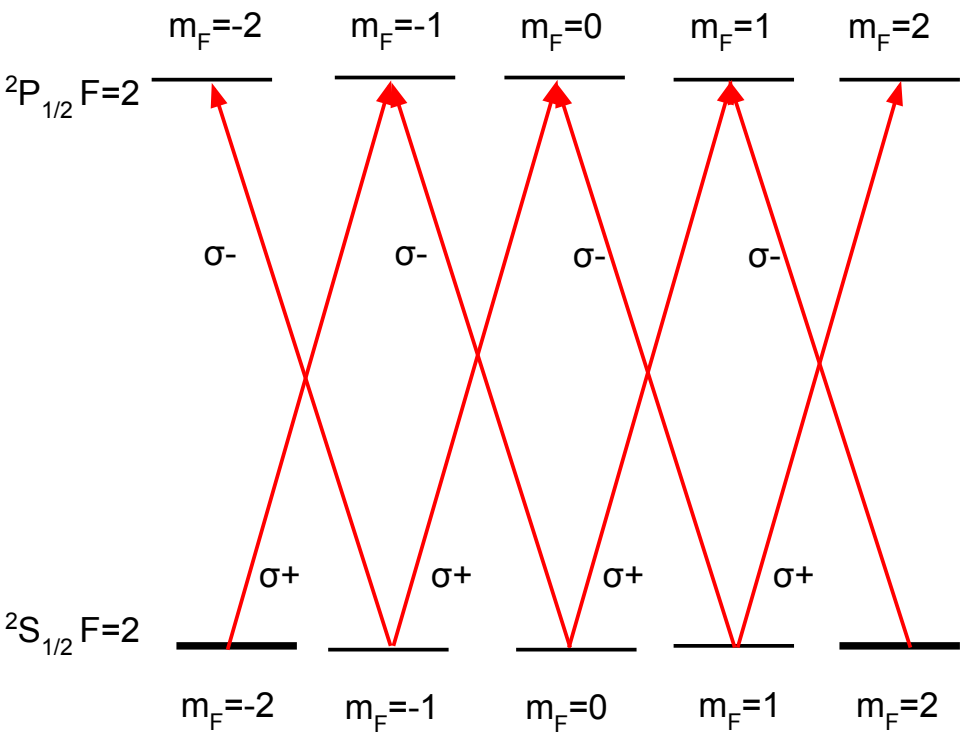

Figure 24: This graph shows the allowed transitions of the D1 line of Lithium 7 using circularly polarized light. The atom in the ${}^2S_{\frac{1}{2}}$ state will be excited by a circularly polarized photon to the ${}^2P_{\frac{3}{2}}$ state. If the incoming light is $\sigma+$ polarized, then the m_F quantum number will increase by 1. If the incoming light is $\sigma-$ polarized, then the m_F quantum number will decrease by 1. The excited atom will emit a photon and return back to the ground state. If the atom emits a $\sigma+$ polarized photon, m_F will decrease by 1 and if the atom emits a $\sigma-$ polarized photon, m_F will increase by 1 to conserve angular momentum. The atom can also emit linearly polarized light, in which case m_F will not change. The polarization of the emitted photon and the subsequent angular momentum of the atom after it has emitted the photon will be determined by Clebsch Gordan coefficients.

photon. The specific angular momentum state the photon is excited to will depend on the polarization of the incoming light.

If the incoming photon has $\sigma+$ polarization, the value of m_F will increase by 1, if it has $\sigma-$ polarization, the value of m_F will decrease by 1 and if it has linear polarization, the angular momentum will not change. The m_F states are degenerate in the absence of a magnetic field, however the degeneracy will be lifted when a magnetic field is applied.

For the transition between the${}^2S_{\frac{1}{2}}, F = 2$ state and the ${}^2P_{\frac{1}{2}}, F = 2$ state, if an atom is in either the ${}^2P_{\frac{1}{2}}, F = 2 m_F = 2$ or $m_F = -2$ excited state and emits a linearly polarized photon, it will decay to the ground state with the same m_F. If the atom is in the ground state with $m_F = 2$, the atom will be unable to absorb a $\sigma+$ polarized photon because it coan not gain further angular momentum and if the atom has $m_F = -2$, it will be unable to absorb a $\sigma-$ polarized photon, because the atom cannot lose further angular momentum. In the magneto-

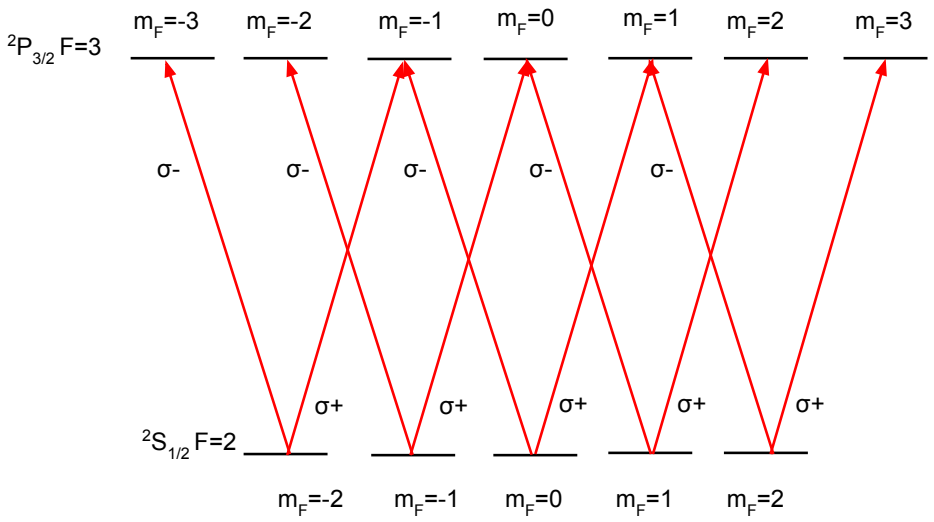

Figure 25: This chart shows the allowed transitions of the D2 line of Lithium 7 using circularly polarized light. Because the total atomic angular momentum F is greater for the excited state than for the ground state, there are no dark ground states. Each ground state can be excited to the upper state using either $\sigma+$ or $\sigma-$ polarized light.

optical trap, one beam will be $\sigma+$ polarized and the other will be $\sigma-$ polarized. Each beam will only interact with atoms traveling opposite the direction of the atomic beam, due to the Doppler shift. Therefore if an atom in the ground state with $m_F = 2$ is traveling in the direction opposite the $\sigma+$ beam, it will be unable to interact with the $\sigma+$ beam because its angular momentum cannot be increased and unable to interact with the $\sigma-$ beam because it is Doppler shifted away from the resonant frequency. The reverse is true for atoms with $m_F = -2$. Because atoms in these states cannot interact with the light, they are considered dark states.

For this reason, the magneto-optical trap will be tuned to the D2 line between the $^2S_{\frac{1}{2}}$, $F = 2$ and $^2P_{\frac{3}{2}}$ $F = 3$. The benefit of the D2 line is that the quantum number F is greater for the excited state than the ground state. This means that for every ground state, the atom can be excited to the excited state by a photon of either $\sigma+$ or $\sigma-$ photons. Unfortunately, the hyperfine states of the ^{7}Li $^2P_{\frac{3}{2}}$state are unresolved, therefore a finite proportion of the transitions from the $^2S_{\frac{1}{2}}$, $F = 2$ states will end in the $^2P_{\frac{3}{2}}$, $F = 2$ state instead of the $^2P_{\frac{3}{2}}$, $F = 3$. This transition has the same deficiencies as the the D1 transition, because atoms in the ground state with $m_F = 2$ and $m_F = -2$ will be invisible to $\sigma+$ and $\sigma-$ light respectively. This problem can be mitigated by using a repumping laser to excite atoms in a dark state back into a state which interacts with the laser light.

5 Conclusion

In this thesis, I have described a method used for cooling and trapping lithium atoms using a magneto-optical trap. The first step of the process is to evaporate solid lithium in an oven to 450° Celsius. The atoms leave the oven through a nozzle, then travel through a high vacuum chamber towards the ultra high vacuum chamber. After leaving the oven, the atoms are collimated into a beam using transverse cooling. The transverse cooling apparatus consists of cage mounted optics designed to aim two elliptically shaped beams through the atomic beam before being retroreflected. Each set of counter-propagating beams are arranged to have orthogonal polarizations in order to create a lin $\perp$ lin profile, which collimates the atomic beam more effectively than randomly polarized beams. The atomic beam then travels through a Zeeman slower, which slows the longitudinal velocities of the atom by using a counter-propagating laser and a spatially varying magnetic field to provide a longitudinal slowing force against the direction of the atomic beam. After exiting the Zeeman slower, the atoms undergo a second round of transverse cooling prior to entering the vacuum main chamber.

In the vacuum main chamber, the atoms will be trapped and cooled using three sets of counter-propagating laser beams and an overlaying magnetic quadrupole field. The counter-propagating beams are circularly polarized with opposite polarizations to create a spatially varying electric field and to allow the atoms to transition to greater total angular momentum. The lasers provide a force against the direction of motion of the atoms because they are detuned by one half the line width so as to interact only with atoms moving against the direction of the laser. The magnetic field is designed to shift the resonant frequencies of the atomic transitions such that the laser is more likely to interact with atoms on the same side of the origin as the laser, providing a net force back towards the origin.

Once the atoms are trapped inside the magneto-optical trap, the magnetic field is switched off and new laser beams are used to trap the atoms in an optical lattice. These beams are aimed at the center of the vacuum main chamber by means of a moveable, pneumatic actuated mirror that can allow either the magneto-optical trap beams or lattice beams through and deflect the other. Once trapped in the optical lattice, the atoms will form a state of matter in which the majority of atoms are in the degenerate ground state. Our lab hopes to run quantum simulations on the trapped atoms to simulate properties of condensed matter physics.

References

[1] Townsend, C. G., Edwards, N. H. Cooper, C. J. Zetie, K. P. and Foot, C. J. Phase Space Density in the Magneto-Optical Trap, 1995, Physical Review A, v. 52 No. 2

[2] Cohen-Tannoudji, C. and Guery-Odelin, D. Advances in Atomic Physics. London: World Scientific Publishing Company, 2011. Print

[3] "Press Release: The 1997 Nobel Prize in Physics". Nobelprize.org. 1 Jun 2013 http://www.nobelprize.org/nobel_prizes/physics/laureates/1997/press.html

[4] Castin, Y. Wallis, H. and Dalibard, J. 1989, Limit of Doppler Cooling. Journal of the Optical Socity of America v.6, No. 11

[5] Raab, E.L. Prentiss, M. Cable, A. Chu, S. Pritchard, D. E. 1987, Trapping of Neutral Sodium Atoms Using Radiation Pressure, Physical Review Letters v. 59, No. 23

[6] Mohan, M. Current Developments in Atomic, Molecular and Chemical Physics with Applications. New York: Kluwer Academic/Plenum Publishers, 2002. Print

[7] Harris, M. L. Design and Construction of an Improved Zeeman Slower. Trinity College Department of Physics, 2003

[7] Lindquist, K. Stephens, M. Wieman, C. Experimental and Theoretical Study of the Vapor-Cell Zeeman Optical Trap, 1992, Physical Review A, v. 46 No. 7

[8] Meyrath, T. Electromagnet Design Basics for Cold Atom Experiments, University of Texas, Austin, Center for Nonlinear Dynamics, 2003

[9] Herzberg. Gerhard, Atomic Spectra and Atomic Structure, 2nd Ed., Dover 1944

[10] Autler, S. H. and Townes, C.H. 1955, Stark Effect of Rapidly Varying Fields, Physical Review, v. 100, No. 2

[11] Wineland, D.J. Sisyphus Cooling of a Bound Atom, 1991, Journal of the Optical Society of America, v. 9 No. 1

[12] Davis, K. B. Mewes, M. O. Ketterle, W. An Analytical Model for Evaporative Cooling of Atoms, 1994, Applied Physics B, v. 60

[13] Carr, A. V. Hyperfine Studies of Lithium Vapor Using Saturated Absorption Spectroscopy, University of Arizona, Department of Physics, 2007

[14] Griffiths, Introduction to Quantum Mechanics. Upper Saddle River, NJ: Pearson Education,1995. Print

[15] Gehm, Properties of ^{6}Li, North Carolina State University, Department of Physics, 2003